https://doi.org/10.1016/j.apenergy.2016.08.180 This is the Pre-Published Version.

Developing a meta-model for sensitivity analyses and prediction of building performance for passively designed high-rise residential buildings

Xi Chen [a*], Hongxing Yang [a] and Ke Sun [b]

[a] Renewable Energy Research Group (RERG), Department of Building Services Engineering, The Hong Kong Polytechnic University, Kowloon, Hong Kong, China
[b] The State Key Laboratory of Refractories and Metallurgy, Wuhan University of Science and Technology, Wuhan, China

Abstract

This paper aims to develop a green building meta-model for a representative passively designed high-rise residential building in Hong Kong. Modeling experiments are conducted with EnergyPlus to explore a Monte Carlo regression approach, which intends to interpret the relationship between input parameters and output indices of a generic building model and provide reliable building performance predictions. Input parameters are selected from different passive design strategies including the building layout, envelop thermophysics, building geometry and infiltration & air-tightness, while output indices are corresponding indoor environmental indices of the daylight, natural ventilation and thermal comfort to fulfil current green building requirements. The variation of sampling size, application of response transformation and bootstrap method, as well as different statistical regression models are tested and validated through separate modelling datasets. A sampling size of 100 per regression coefficient is determined from the variation of sensitivity coefficients, coefficients of determination and prediction uncertainties. The rank transformation of responses can calibrate sensitivity coefficients of a non-linear model, by considering their variation obtained from sufficient bootstrapping replications. Furthermore, the acquired meta-model with MARS (Multivariate Adaptive Regression Splines) is proved to have better model fitting and predicting performances. This research can accurately identify important architectural design factors and make robust building performance predictions associated with the green building assessment. Sensitivity analysis results and obtained meta-models can improve the efficiency of future optimization studies

* Corresponding author: Tel.:+852-2766 4726, Fax: 2765 7198, E-mail: climber027@gmail.com
The short version of the paper was presented at CUE2015 on Nov. 15-17, Fuzhou, China. This paper is a substantial extension of the short version.

by pruning the problem space and shorten the computation time.

Keywords: Meta-model; Indoor environment; Regression analysis; Passive design; Bootstrap

1. Introduction

Green building rating schemes emerged in the 1960s as potential methods to improve the building sustainability from multiple aspects including the energy efficiency, material use, and indoor environment quality [1-4]. Given the fact that building sectors account for over 60% of total energy consumption in Hong Kong, BEAM (Building Environmental Assessment Method) has been practiced by researchers, designers and engineers for two decades to encourage the environmental awareness of the construction industry [5, 6]. Especially, Hong Kong Housing Authority is taking a leading role to build BEAM certified high-rise residential buildings to accommodate nearly one third of the local population. In a recent update of this local green building rating scheme, passive design strategies are proposed to maximize their influences over the building sustainability from the earliest construction stage [7, 8]. Passive designs covering the building layout, envelop thermophysics, building geometry and infiltration & air-tightness have been proved to significantly affect building performance in previous regression analyses [9-12]. These analyses can not only interpret the relative importance of each design strategy (i.e. the sensitivity analysis), but also predict future building performance (i.e. statistical modelling). Both the sensitivity analysis (SA) and statistical modelling can assist decision-makers in the initial stage of a construction project to efficiently deploy their resources over green building features.

1.1.Sensitivity analysis

The sensitivity analysis is widely applicable to relating input parameters with the overall building performance [13]. The unique contribution from each input can be determined by SA to prepare for future optimization of energy, environment and economic performances [14, 15]. SA methods can usually be classified to the local SA where input parameters are varied one at a time and the global SA where all inputs are changed simultaneously [16-18]. The local SA is used to examine the energy performance of office buildings in Hong Kong with the DOE-2 program. Input factors of building loads, HVAC systems and refrigeration plants were varied separately to examine their influences over building energy consumption, the peak design load and annual load profiles. As a

result, the lighting load, thermal setpoint and chiller coefficient of performance were proved to be most important design parameters in each category [17]. The optimum slab thickness of floors, ceilings and external walls was determined based on a local sensitivity analysis of the building envelop, where the maximum window to wall ratio was expressed by a function of the diurnal temperature amplitude [19]. The window aperture area was also independently correlated with the peak electricity demand and annual energy consumption to provide simple design charts for engineers in early planning stages [20]. Apart from the above architectural features, shading effects from the balcony and surrounding structures were independently investigated by local SAs [21, 22]. On the other side, the global SA is adopted to study the uncertainty and sensitivity of a passively cooled office building in moderate climates [23]. The impact of single-sided ventilation, passive stack and cross ventilation strategies on indoor thermal comfort conditions was investigated in this research, where the single-sided ventilation contributed to the largest uncertainty in the model output. In addition, design guidelines for conducting sensitivity studies on the total annual energy consumption of low-rise residential buildings are developed in a background of global warming [24, 25]. The natural ventilation, window area, and solar heat gain coefficient are founded to be the most important design parameters in such buildings. However, the uncertainty of natural ventilation can be attributed to more elementary building designs such as window properties and opening configurations [26, 27].

1.2.Statistical modelling

The statistical modelling is another application of regression analyses, in which meta-models (or surrogate models, emulators etc.) are developed from either monitored building operation data or simulation cases from detailed engineering models [28]. Campus building stock data were used to construct statistical energy meta-model with both linear and non-parametric regression approaches [29]. In this study, linear models showed better prediction performances through a simple transformation of response data. Measured data of these buildings were also used to predict the base temperature and enthalpy with multiple linear regression analyses [30]. Hilliard et al. developed a predictive control strategy for a college building with the combination of EnergyPlus and R software. The deadband setpoint strategy performed better as a comfort maintenance measure compared to the fixed setpoint strategy in terms of energy reduction [31]. A Brazilian meta-model for both naturally

and artificially ventilated residential buildings was developed from EnergyPlus simulations, where the artificial neural network model outperformed multiple regression models under a local energy labelling system [32]. In addition, Fan et al. proposed a data-mining method to develop an ensemble model for predicting the future energy consumption and peak demand [33]. The model was successfully applied to the tallest building in Hong Kong and was valuable for the fault detection and diagnosis as well as operation optimization.

According to the above introduction and literature review, it can be recognized that little existing research focuses on developing meta-models for passively designed high-rise residential buildings in hot and humid climates. Such studies should include a comprehensive statistical analysis on the model interpretation and prediction. This paper mainly focuses on the regression analysis of a generic building model with selected passive design parameters under a free-running mode. Miscellaneous internal loads and operational controls are excluded from the modelling process to observe the unique influence of the passive design on indoor environmental performances. Unlike most existing studies, the natural ventilation rate is treated as a model output to evaluate the impact of elementary architectural designs. The thermal comfort performance is another model output in the unconditioned building to represent the time when cooling energy consumption can be exempted, while the daylight performance is presented to indicate the time when artificial lighting can be waived with a specified illuminance threshold. The sampling size, resampling method, rank transformation, and different statistical models are thoroughly investigated by massive modelling experiments to obtain calibrated sensitivity coefficients and robust surrogate models.

2. Research design and methodology

This study intends to perform an in-depth statistical regression analysis between passive design parameters and indoor environmental conditions. On top of previously conducted sensitivity studies [10], influences of sampling sizes on SA indices, applications of resampling methods, and comparisons between different statistical models are conducted according to illustrations in Fig. 1. A generic model representing a typical high-rise residential building in Hong Kong is first constructed to simulate the daylight, natural ventilation and thermal comfort performance. The Monte Carlo Analysis is then adopted to generate the input-output matrix for regression analyses. Furthermore, an appropriate sampling size is determined with stabilized statistical estimators and clearly identified

distribution patterns. Different regression models are applied to the sensitivity analysis and statistical modelling, where the optimized model is bootstrapped and cross-validated to assess the variation of sensitivity coefficients and uncertainty of model predictions.

2.1.Building modeling and input variation

The Public Rental Housing (PRH) is a typical high-rise building developed by the Hong Kong Housing authority for low-income local residents. These buildings are modularly designed with typical layout plans shown in Fig. 2. Private flats are located in the perimeter zone of a typical floor to allow the penetration of daylight and natural ventilation. In building performance simulations, the typical floor model can represent the whole building for the sake of time-saving in a large-sample modelling experiment [34]. Therefore, a two-habitant hypothetic generic model in the center of the typical floor is constructed to represent the worst-case scenario for the daylight and ventilation access. The model is assumed to be unoccupied to exclude influences from residents and operating schedules. Its physical parameters are in compliance with the local construction practice and green building standard as summarized in Table 1 [8].

The indoor environmental solutions of the generic model are obtained from interlinked sub-modules in EnergyPlus, which has been extensively recognized, calibrated and validated in building performance analyses [35, 36]. The indoor illuminance level was calculated by the combination of sky component, shading and daylight sub-modules based on the room geometry, window transmittance and wall surface property, while ventilation and thermal conditions are derived from heat balance and airflow network sub-modules [37].

2.1.1. Daylight calculation

Daylight calculation is performed whenever accessible to the sunlight with a reference sensing point specified in the middle of the room. The interior illuminance at the reference point is calculated by multiplying the daylight illumination factor for the current solar position with the external horizontal illuminance from the weather file. The calculation process for each time step can be expressed by Eq. (1) to Eq. (3):

$$\bar{d}_{sun}(i_L, i_S) = w_j d_{sun}(i_L, i_S, i_h) + (1 - w_j) d_{sun}(i_L, i_S, i_h + 1) \quad (1)$$

$$E_{h,sun} = \eta_{dir} S_{norm,dir} \cos Z \quad (2)$$

$$I_{win}(i_L, i_S) = \bar{d}_{sun} E_{h,sun} \quad (3)$$

where $\bar{d}_{sun}(i_L, i_S)$ is the daylight illuminance factor; i_L is the reference point index; i_S is the window shade index (1 for unshaded window); i_h is the hour number; w_j is the weighting factor for the time-step interpolation; $E_{h,sun}$ is the exterior horizontal solar illuminance; Z is the solar zenith angle; η_{dir} is the luminous efficacy of direct radiation from the sun; $S_{norm,dir}$ is the direct normal solar irradiance; and $I_{win}(i_L, i_S)$ is the interior illuminance from a window.

2.1.2. Airflow network algorithm

Airflow network (AFN) algorithm is adopted to simulate the single-sided natural ventilation, where airflow is driven by the synergy of the wind pressure and buoyancy through cracks and windows. In AFN, the flowrate is derived from the pressure difference between thermal zones, and the resultant thermal load is further combined with original air balance equations to acquire the final indoor condition. Airflow patterns through the vertical window vary according to the height of the neutral plane [38], and the total flowrate can be calculated as a function of the height h by Eq. (4) in the one-way flow condition, and Eq. (5) and (6) in the two-way flow situation:

$$\dot{m}_{0,H} = C_d \theta \int_{h=0}^{h=H} \rho v(h) \mathrm{W dh} \quad (4)$$

$$\dot{m} = C_d \theta \int_{h=0}^{h=Y} \rho v(h) \mathrm{W dh} \quad (5)$$

$$\dot{m} = C_d \theta \int_{h=Y}^{h=H} \rho v(h) \mathrm{W dh} \quad (6)$$

where θ is the opening area reduction factor (dimensionless); ρ is the air density; C_d is the discharge coefficient (dimensionless); H is the height of the window; W is the window width; and Y is the height of the neutral plane (with zero airflow speed).

The calculation of indoor heat and moisture balance adopts a predictor-corrector approach, in which the heat and air mass balance is a summary of internal latent loads, infiltrations, air systems, multi-zone airflows and convections on zone surfaces. The mean zone operative temperature can be expressed by Eq. (7) and (8):

$$\rho_a C_p C_T \frac{dT_z}{dt} = \sum_{i=1}^{N_l} Q_i + \sum_{i=1}^{N_{surf}} h_i A_i (T_{si} - T_z) + \sum_{i=1}^{N_{zone}} m_i C_p (T_{zi} - T_z) + m_{\inf} C_p (T_\infty - T_z) \quad (7)$$

$$T_o = \gamma T_z + (1-\gamma)\overline{T_r} \quad (8)$$

where A_i is the area of room surfaces; C_p is the zone air specific heat; C_T is the sensible heat capacity multiplier; h_i is the convective heat transfer coefficient; m_i is the inter-zone air mass flow rate; m_{inf} is the infiltration air mass flow rate; N_l is the number of latent internal loads; N_{surf} is the number of zone surfaces; N_{zone} is the number of zones; Q_i is the convective internal loads; T_o is the operative temperature; T_{si} is the temperature of zone surfaces; T_{zi} is the mean temperature of i^{th} zone; T_z is the zone air temperature; $\overline{T_r}$ is the mean radiant temperature; T_∞ is the temperature of the outdoor air; γ is the coefficient depending on the relative air speed according to ASHRAE 55; and ρ_a is the zone air density. With similar principles, the zone humidity ratio is defined as Eq. (9):

$$\rho_a V_z C_W \frac{dW_z}{dt} = \sum_{i=1}^{N_l} kg_i + \sum_{i=1}^{N_{surf}} \rho_a h_{mi} A_i (W_{si} - W_z) + \sum_{i=1}^{N_{zone}} m_i (W_{zi} - W_z) + m_{\inf} C_p (W_\infty - W_z) \quad (9)$$

where C_W is the humidity capacity multiplier; h_{mi} is the convective mass transfer coefficient; kg_i is the internal moisture loads; V_z is the zone volume; W_{si} is the humidity ratio of zone surfaces; W_{zi} is the humidity ratio of i^{th} zone; W_z is the zone air humidity ratio; and W_∞ is the humidity ratio of the outdoor air.

In this study, a "simple opening" component with a constant air mass flow exponent of 0.65 represents the large vertical window opening on the external wall. The crack component adopts the same exponent setting as the window. Openable windows are controlled to allow natural cooling whenever the indoor temperature is higher than that of the outdoor.

2.1.3. ASHRAE 55 comfort model

The ASHRAE Standard 55 adaptive model of the 90% acceptability is selected to assess the indoor operative temperature under naturally ventilated conditions for hot and humid climates according to previous research conducted by the authors. The 90% acceptability limits of the operative temperature are defined by Eq. (10) and (11) [39]. The proportion of time in the cooling period when the indoor temperature falls within the limits is then taken as the comfort index.

$$T_{o,up90} = 0.31 T_{ao} + 20.3 \quad (10)$$

$$T_{o,low90} = 0.31T_{ao} + 15.3 \quad (11)$$

where $T_{o,up90}$ is the upper limit of acceptable operative temperature; $T_{o,low90}$ is the lower limit of acceptable operative temperature; and T_{ao} is the prevailing mean outdoor air temperature.

2.1.4. Weather conditions and input variations

Climatic conditions can greatly impact indoor environmental conditions because the variation of the outdoor temperature, humidity, radiation and wind speed to can greatly impact the effectiveness of passive design strategies [40-42]. In this research, Hong Kong (22.3 Nº, 114.17 Eº) is chosen as a representative city in hot and humid subtropical climatic regions to investigate the building performance in cooling periods. According to recommendations from the local green building guidance, the use of air-conditioning in Hong Kong usually lasts from April to October with the peak load in July and August [43]. However, April can be excluded by observing the electricity consumption trend of local buildings when the ASHRAE 90% acceptability model is used to assess thermal comfort conditions under natural ventilation conditions [42, 44].

Passive design parameters are treated as model inputs in this study and their variation ranges are determined with reference to local building practices and engineering experiences (see Table 2). These strategies with potential influences over the future cooling and lighting energy consumption, are specified as the external obstruction angle (EOA), building orientation (BO), wall thermal resistance (WTR), wall specific heat (WSH), window U-values (WU), solar heat gain coefficient (SHGC), visible light transmittance (VLT), window to ground ratio (WGR), overhang projection fraction (OPF) and infiltration air mass flowrate coefficient (IAMFC). These input variables are varied uniformly within their distribution ranges. EOA is introduced to measure surrounding obstructions as defined in previous research [45, 46], where the upper limit of 87 is assumed with a typical building height of 100 m and a minimum road width of 5 m as per the Building Ordinance in Hong Kong. The design domain of WTR, WU and WTH is recommended by EnergyPlus manuals [37]. VLT is controlled to vary synchronously with SHGC and only impacts daylight performances. In addition, the lower limit of WGR is set to meet the minimum glazing size required by PNAP APP-130.

2.2.Statistical regression analysis

In this research, the regression analysis begins with the Monte Carlo method, which basically utilizes computer generated random variables to approximate univariate and multidimensional integrals [47]. An adequate sample size has to be determined first for either the sensitivity analysis (SA) or statistical modelling based on the stability of estimators and prediction residuals. Then the statistical training of different regression models is conducted on the input-output dataset. Finally, bootstrapping and cross-validation is applied to obtain more complete and robust information about sensitivity indices and prediction accuracies.

2.2.1. Generating the input-output matrix

The sampling-based Monte Carlo method is a technique that operates a model multiple times with random samples generated from input distributions. It provides approximate solutions to both uncertainty and sensitivity analyses by performing statistical modelling experiments [48, 49]. The method can handle complex black-box models irrespective of the linearity and continuity, and generate a probability distribution for each output depending on input distribution types [16].

Monte Carlo method can be combined with the Latin Hypercube Sampling (LHS), which is famous for its brief concept, convenient implementation, and effective stratification across the whole distribution range of variables [50]. To derive the proper size of training data for regression analyses, changing sample sizes from 100 to 10000 are produced with LHS according to Table 2 [51]. Building simulations are then conducted to obtain indoor environment indices including the illuminance level (IL), air change rate (ACR) and ASHRAE55 comfort time (ACT). The whole process can be summarized by the following equation:

$$\vec{Y} = \begin{bmatrix} y_1 \\ y_2 \\ \vdots \\ y_N \end{bmatrix} = \begin{bmatrix} f(x_{11}, x_{12}, \cdots, x_{1k}) \\ f(x_{21}, x_{22}, \cdots, x_{2k}) \\ \vdots \\ f(x_{N1}, x_{N2}, \cdots, x_{Nk}) \end{bmatrix} \tag{12}$$

where N is the sample size; k is the number of input factors; x is the input variable; and y is the output variable.

2.2.2. Sensitivity analysis

The sensitivity analysis (SA) is performed to determine the contribution of each input parameter to the variance of specified outputs of the building model. SA is valuable for both modelling and experimental studies when exploring building physical responses to changing design and operation

conditions [13]. It can usually be divided to two categories: the local sensitivity analysis and global sensitivity analysis. The local SA, as introduced in Section 1, is quite straightforward and time-saving but highly dependent on the controlled value of other variables, addressing little interaction between input variables [18]. On the other side, the global SA can evaluate output responses by varying all input variables at the same time and is thus selected to conduct following regression analyses.

One sensitivity index used in this research is the standardized regression coefficient (SRC). It is obtained from a multiple linear regression model when the input-output matrix has been standardized. The absolute value and sign of SRC indicate the relative importance of each input and the changing direction of the output against the input. A common multiple linear regression analysis of responses/outputs (y_i) and inputs/predictors (x_i) takes the form of Eq. (13):

$$\hat{y}_i = \beta_0 + \sum_{j=1}^{k} \beta_j x_j \tag{13}$$

where $\hat{y}_i$ is the predicted y_i by the model; and β_j is the regression coefficient determined by minimizing Eq. (14):

$$\sum_{i=1}^{N} (y_i - \hat{y}_i)^2 = \sum_{i=1}^{N} \left[y_i - \left(\beta_0 + \sum_{j=1}^{k} \beta_j x_{ij} \right) \right]^2 \tag{14}$$

The sensitivity coefficient (SRC) of each predictor in the regression model can be calculated by:

$$SRC_j = \frac{\beta_j \sigma_x}{\sigma_y} \tag{15}$$

$$\sigma_x = \left[\sum_{i=1}^{N} \frac{(x_{ij} - \bar{x}_{ij})^2}{N-1} \right]^{1/2} \tag{16}$$

$$\sigma_y = \left[\sum_{i=1}^{N} \frac{(y_i - \bar{y}_j)^2}{N-1} \right]^{1/2} \tag{17}$$

where $\bar{x}_{ij}$ and $\bar{y}_j$ are the averaged input and output respectively.

The coefficient of determination (R^2) is further formulated by Eq. (18) to assess the correlation between the input and output. A value higher than 0.7 is preferred so that the acquired model can explain most of the variation in outputs [16].

$$R^2 = \frac{\sum_{i=1}^{N} (\hat{y}_i - \bar{y})^2}{\sum_{i=1}^{N} (y_i - \bar{y})^2} \tag{18}$$

Apart from R^2, the variance inflation factor (VIF) has to be computed to detect the existence of multicollinearity between three or more input parameters (see Eq. (19)). Some input parameters might be correlated with others in building performance analyses such as the natural ventilation rate and window area which are both used as inputs in some studies [24, 25]. The smallest value of VIF is 1, indicating the complete elimination of collinearity.

$$VIF = \frac{1}{1 - R^2_{x_j | x_{\_j}}} \tag{19}$$

where $R^2_{x_j | x_{\_j}}$ is the R^2 from a regression of x_j on all other predictors. In this study, VIF of all selected inputs is within 1.02, suggesting an almost non-correlated dataset.

The other sensitivity coefficient calculated from the multiple regression analysis is the Standardized Rank Regression Coefficient (SRRC), which is SRC after the rank transformation of outputs or/and inputs. It can improve the linearity and R^2 of the regression model [52]. Rank transformations provide a robust and useful solution in the case of long tailed input and output distributions with an appropriate low association index [53].

2.2.3. Bootstrapping in sensitivity analysis

The bootstrap method can evaluate the accuracy of an estimator (e.g. the sensitivity coefficient and root mean square error) by a random resampling with the replacement from the original dataset [28]. It involves the application of the plug-in principle, where the original probability distribution function F ($\theta = t(F)$) of an estimator θ is replaced by the same empirical distribution function $\hat{F}$ ($\hat{\theta} = t(\hat{F})$) of a corresponding $\hat{\theta}$ [54]. The empirical distribution $\hat{F}$ is defined by a discrete distribution which puts an equal probability to each sample value in the dataset.

Fig. 3 explains the working principle of a bootstrapping process. An original dataset of Z is first created as per Section 2.2.1. Assuming a sample size of 100, Z is then 100 combinations of 10 vectors (i.e. 9 input parameters and 1 output from the building model). An initial bootstrap sample Z^*_1 with the exact same dimension of the original one is then generated by randomly sampling 100 times from the original dataset with replacement. As shown in the flowchart, each vector in the bootstrap sample Z^*_1 can be any element extracted from the original dataset and repetitions of some vectors might be observed. This process is repeated B times until the required number of bootstrap samples is met. An

adequate number of B is reached when the calculated statistical estimator becomes stable [54]. Subsequently, the statistical estimator (i.e. the sensitivity coefficient in this study) $\hat{\theta}^*$ is calculated for each bootstrap sample, and the standard deviation of the estimator can be acquired from Eq. (20) [55]:

$$S_{\hat{\theta}^*} = \sqrt{\frac{1}{B-1}\sum_{k=1}^{B}(\theta_k^* - \frac{1}{B}\sum_{k=1}^{B}\theta_k^*)^2} \quad (20)$$

The variation of sensitivity coefficient and its confidence intervals can be automatically estimated by the least-square method if only the following assumptions are not violated: a) The predictors are observed without errors; b) the error has a finite variance; c) the error is independent of predictors; and d) the error has the same probability distribution for each observation [56]. However, a heavy-tailed residual distribution or a few outliers can easily violate these ideal assumptions. Therefore, the parametric bootstrap should be more reliable in estimating the uncertainty of sensitivity indices.

2.2.4. Statistical modeling and surrogate model selection

The standard regression analysis described in previous sections is used to estimate the relative importance of different input design parameters, while the statistical regression is introduced to develop a refined model for predicting indoor environmental indices instead of the simulation software. In statistical regression analyses, not all inputs are necessary for a meaningful interpretation of outputs. Decisions about which variable is included or omitted from the regression equation are exclusively based on particular sample-drawn statistics where minor differences can have profound influences over the relative importance of an input [57]. There are three common statistical regression methods, namely the stepwise regression, forward selection and backward deletion. The forward selection is a process starting from an empty input subset where new predictors are entered one at a time if correlation-based selection criteria are satisfied. The qualified predictor stays in the regression equation once entered, so that important variables are less likely to be excluded from the prediction model. In the backward deletion, the regression equation starts with all predictors included and removes anyone which is identified as an insignificant contributor to the output variation. The stepwise regression is a combination of the above two selection methods, where the equation begins empty and adds or deletes a new predictor according to its contribution.

Apart from the linear regression model used in SA, a non-parametric model called the

Multivariate Adaptive Regression Splines (MARS) is also used to address any non-linearity observed between inputs and outputs. MARS is a combination of the spline regression, stepwise model fitting and recursive partitioning [58]. It takes the form of Eq. (21):

$$\hat{y}_i = \beta_0 + \sum_{j=1}^{k} \beta_j \phi_j(x_i) \tag{21}$$

where $\phi_j(x_i)$ is the basis function or hinge function defined as:

$$\phi_j(x_i) = \max(x_i - const) \text{ or } \phi_j(x_i) = \max(const - x_i) \tag{22}$$

The constant in Eq. (22) is called knot which divides the distribution range of input variables. The model building process is a similar to that of the stepwise regression starting with an intercept only model where new basis functions are included or excluded based on their impacts on the residual error. The Generalized Cross Validation (GCV) score is then calculated to evaluate the performance of each model:

$$GCV = MSE / (1 - ENP / \mathrm{N})^2 \tag{23}$$

where *MSE* is the mean squared error of a training data in size *N*; and *ENP* is the effective number of parameters.

2.2.5. Cross-validation of surrogate model

As mentioned in Section 2.1.1, the sample for carrying out statistical regression should be sufficiently large and representative because the selection of predictors might depend on minor differences in the statistical significance and the equation from limited samples cannot be generalized to the whole population. In addition, the statistical modelling may not lead to the optimum R^2 value, because a combination of multiple predictors can increase R^2 whereas a single predictor might decrease it. The above problems are generally recognized as the overfitting phenomenon, which can impair the effectiveness of developed surrogate models. In this situation, a cross-validation with a second sample is necessary to obtain a robust prediction equation. In the study, the original sample generated with LHS is used as the training set to produce the equation, while the other randomly generated sample of an equal size is used to examine its validity. The Root Mean Square Error (RMSE) is then calculated to assess the prediction accuracy as per Eq. (24):

$$RMSE = \sqrt{\frac{\sum_{i=1}^{N}\left(y_i - \hat{y}_i\right)^2}{N}} \quad (24)$$

3. Results and discussions

This research involves the sensitivity analysis (SA) and statistical modelling of a typical high-rise residential building under natural ventilation and lighting conditions with passive design strategies as predictors and indoor environmental indices as responses (i.e. the illuminance level, air change rate and AHREA55 comfort time). The influence of the sampling and resampling size (bootstrapping), the response transformation and comparisons between different regression models are thoroughly investigated. The main findings and correlations with existing studies are presented in this section.

3.1. Impact of sampling size on the linear model

The target of this section is observing the influence of sampling size on multiple linear regression models for indoor environmental outputs and deciding the adequate sample size to obtain stable statistical estimators and test the hypothesis of input parameters. For this purpose, the LHS sampling size has been changed from 100 to 10000. Multiple model estimators including SRC, R^2 and RMSE are calculated for each regression trial to observe their variations, while residual plots are presented to highlight the response-predictor relationship.

Fig. 4 shows the variation of SRC for each predictor of the daylight performance over the sampling range. It can be clearly seen that SRCs are stabilized by an increasing sample size. When starting with a small sample size of 100, VLT (visible light transmittance), WGR (window to ground ratio), EOA (external obstruction angle) and OPF (overhang projection fraction) are obviously more important than other design parameters. SRCs of other design parameters are either around or lower than 0.1 with less impact on the illuminance level. Trade-offs between rankings of the four important inputs and others are identified in regression trials with a sample size smaller than 800. For instance, EOA ranked fourth after OPF at an initial sample size of 100, but its importance exceeded OPF as the sample size grew to 200 and 400. However, when the sample size exceeded 600, the two parameter started making almost equal contributions to the variation of daylight performances. On the other side, BO (building orientation) was initially the fifth influential factor but become less important with an enlarged sample size from 100 to 600. These variations of SRCs wear off when the sample size is over 800. VLT stays to be the most important input throughout regression trials with a final sensitivity

index of 0.580, while WGR ranks behind it with a SRC of 0.438. EOA and OPF are almost equally important predictors with final SRCs of 0.276 and 0.265. Based on the above statistical analysis, stabilized SRCs can only be obtained with a sample size larger than 800. Besides sensitivity coefficients of input factors, the calculated RMSE and R^2 of the regression model also varied with the sampling size as shown in Fig. 5. RMSE of the model was stabilized to around 160.000 after the sample size exceeded 600. Similarly, R^2 value dropped from 0.740 to a stable level between 0.670 and 0.703 when the sample size was over 600. Another important indicator varying with the sampling size is residual statistics, namely its distribution pattern and correlation with predicted responses. As mentioned in Section 2.2.3, the linear regression assumes homoscedastic, independent and normally distributed error terms, which can be examined by the scatterplot of standardized residuals. A discernible distribution pattern is recognized when the sample size reaches 600, and a smooth fitted line of residuals can help to discover the pattern based on smaller sample sizes. The conspicuous U-shape of residuals indicates a deviation from normal distribution and non-linear relationship between predictors and responses (See Fig. 6).

SRCs for the natural ventilation index also varies with the sampling size (as shown in Fig. 7). WGR, SHGC and IAMFC (infiltration air mass flow coefficient) are constantly the three most important design parameters, whose SRCs are finally stabilized to approximately 0.814, 0.449 and 0.193 respectively. Besides these important factors, the sensitivity ranking of BO and WU changed dramatically in smaller sample sizes (i.e. from 100 to 200). The variation of remaining inputs is not conspicuous and their impacts on the air change rate are relatively weak. Judging from the overall variation of SRCs and their rankings, a sampling size of 600 should be adequate to carry out robust sensitivity analyses on the natural ventilation performance. Furthermore, the variation of RMSE and R^2 versus the sampling size is presented in Fig. 8. RMSE becomes steady after the sample size exceeds 600, while R^2 for the regression model stays constant at a level between 0.911 and 0.931 irrespective of sampling sizes. As a result of above analyses, a sample size over 600 can lead to a robust training model for the air change rate (ACR). In addition, the residual distribution is expressed in Fig. 9, where scattered points take the same U-shape as suggested by the smooth fit line. The pattern is quite clear from the beginning of the sampling process, and the assumption of normal distribution is obviously violated.

Similar to the illuminance level and air change rate, the variation of the sample size was conducted on the regression model for thermal comfort (i.e. ASHRAE55 comfort time). As presented in Fig. 10, the variation of SRCs is minimized with growing sample sizes. SHGC, WGR, EOA and OPF are again evaluated as the four most influential predictors, whose SRCs eventually converge to 0.774, 0.425, 0.205 and 0.145. SRCs of remaining inputs are uniformly lower than 0.100 with less impact on the ACT. BO was initially the fifth influential factor but became insignificant with larger

sample sizes. Trade-offs between sensitivity rankings only exist in less important predictors, whose variations are also minimized after the sample size exceeds 1000 (i.e. a sufficient sample size to acquire stable SA results). Unlike SRCs, RMSE and R^2 remain steady throughout the whole range of the sampling size (see Fig. 11), and residual plots are pattern free compared to the former two regression models (see Fig. 12). Nevertheless, the histogram and normal P-P plot of standardized residuals are further analyzed to confirm the normality of error distributions in Fig. 13. The distribution mass for 1000 samples is slightly left concentrated so that the error distribution is right-skewed. The skewness can be identified from the slightly S-shaped curve in the normal P-P plot as well.

In summary, a sample size of 1000, which is equivalent to 100 samples per model input, should be large enough to make robust statistical estimation with linear regression models for indoor environmental outputs. With this number of samples, the normality of error distribution can also be clearly determined from residual plots without fitted lines. The derived sample size, which is far above minimum simulation runs (e.g. 10 or 15 runs per input parameters) recommended by existing sensitivity analyses [25], proves the necessity of performing this procedure before starting regression analyses. To be best knowledge of authors, only Tian et al. conducted a similar study to determine the required sampling number for conducting SA on annual building energy consumption and carbon emissions. The determined sample size from their study was only 500, which is considered inadequate to generate stable statistics of regression models [28]. Furthermore, R^2 and the distribution pattern of residual plots are also used in determining the required minimum sample size in this study, where a comprehensive approach for regression analyses is formulated.

3.2. Rank transformation in the linear model

As determined from the previous sampling test, a sufficient sample size of 1000 is determined for further statistical analyses. Because the non-linearity in the dataset can impair the prediction accuracy and other findings from the fitted model, the rank transformation is applied to model responses to reduce the non-linearity detected by residual plots. The change of sensitivity coefficients and residual distributions are highlighted in this section.

Fig. 14 compares the residual plots of the rank transformed model with the original model for the daylight performance. The right scatterplot shows more evenly distributed residuals around the zero line, indicating a successful transformation of the response. The sensitivity coefficient (SRRC)

458 of newly fitted models is then compared with original models in Fig. 15. Differences between most
459 SRCs and SRRCs of predictors for the daylight performance are within in 1%, causing no significant
460 changes in their relative importance. However, the sensitivity index of EOA increased by 5% with
461 rank transformations while the sensitivity index of OPF dropped by 6%, leading to an exchange of
462 their rankings in the order of importance. The results also indicate that rank transformations can
463 calibrate the regression indices when non-linearity is observed between inputs and outputs.
464 Transformation results for natural ventilation and thermal comfort models are also summarized in
465 Table 3, in which all sensitivity coefficients for these two models are subject to minor changes within
466 2%.
467 Compared to the quadratic and square root transformations conducted in a related study [29],
468 the rank transformation is capable of improving the SA performance in a more efficient approach.
469 Obtained sensitivity indices can also be incorporated into the passive design criteria of green building
470 rating schemes to create a statistically robust credit weighting system [8, 43].
471
472 **3.3. Bootstrapping for regression coefficients**
473 The bootstrap method is further applied to above regression models to acquire the confidence
474 intervals of derived sensitivity coefficients. According to the methodology section, a preliminary
475 analysis is necessary to determine the required number of bootstrap replications. For the sake of
476 saving computation time, the preliminary analysis is applied to a small original dataset containing
477 100 samples. In addition, the Unstandardized Regression Coefficient (URC) is used instead of SRCs
478 and SRRCs to differentiate their scales so that the variation with different bootstrap samples can be
479 easily detected. Taking the daylight model as an example (See Fig. 16), the standard deviation of
480 URCs for VLT, WGR and OPF experienced dramatic fluctuations with less bootstrap replications,
481 but their values became steady once the sample size exceeded 600. These three parameters are also
482 main contributors to the variation of illuminance levels. In contrast, the standard deviation of URCs
483 for other predictors was barely changed by increasing the sample size. The preliminary analysis on
484 the natural ventilation and thermal comfort model expressed similar variations where the standard
485 deviation of UCRs for important predictors converged over 600 bootstrap samples. Consequently,
486 1000 bootstrap replications are applied to SA in this study, where the variation of SRRCs, instead of

a single value in a traditional SA, is presented in Table 4. From the tabular summary, the mean standard error of sensitivity indices for the daylight, ventilation and thermal comfort model is estimated to be 1.7%, 0.8% and 1.2% respectively.

Given the obtained confidence intervals of sensitivity indices for the three regression models, the rank transformed daylight responses can make a statistically significant difference of sensitivity indices (i.e. 6% of OPF and 5% of EOA). Compared to most existing sensitivity studies [16, 23, 25], the probabilistic analysis with the bootstrap method can offer a robust ranking of design factors by clarifying the uncertainty of sensitivity indices.

3.4. Statistical model building and validation

In the aforementioned sensitivity study, all predictors are included in the model equation to investigate their influences over specified indoor environmental outputs. However, in the statistical modeling, their entry to a regression model purely depends on the contribution to statistical estimators (e.g. R^2). According to the comparison in Table 5, four less influential inputs including the WU (window U-value), IAMFC (infiltration air mass flow coefficient), WTR (wall thermal resistance) and WSH (wall specific heat) are removed from the daylight model by a stepwise regression. Although the equation is simplified, it can still explain most of the variations in the output (i.e. R^2 unchanged) with the same prediction accuracy (i.e. RMSE unchanged). In regard of the natural ventilation model, the stepwise regression provides an equation with two items removed: BO (building orientation) and WSH. R^2 and RMSE also maintain at the same level as the standard regression model. When the stepwise algorithm is applied to the thermal comfort model, only BO is absent from the stepwise regression model, which can also make predictions with an equal accuracy. In spite of the model reduction achieved by the stepwise regression, the estimated RMSE accounts for 36.467%, 11.967% and 4.743% of the mean predicted model responses, indicating an unacceptable large uncertainty especially for the daylight and ventilation performance. Therefore, the non-parametric MARS model is applied to further improve the quality of surrogate models.

MARS creates a model in two main steps: the forward pass and backward pass. In the forward pass, new basis functions/items are added to the equation until the model is overfitted based on the same principle in stepwise regression to maximize the R^2 value. In contrast, the backward pass

discards basis functions/items to minimize the GCV value, which is a trade-off between the model flexibility and RSS (Residual Sum-of-Squares). Consequently, this statistical approach can build a regression model with an optimal number of basis functions as well as improved R^2 and RMSE.

The meta-model developed for the daylight assessment takes the form of Eq. (25). The MARS model employs six out of nine input variables with R^2 of 0.766 and RMSE of 137.274, which are both obviously improved from the linear model (R^2 of 0.703 and RMSE of 154.583). Despite the significant improvement, the correlation of predicted and simulated results still deviates largely from the ideal diagonal line in the scatterplot (see Fig. 17). The meaning of each symbol in following equations has been explained in Section 2.

$$\begin{aligned} IL = {} & 820.474405888856 - 709.879726102374 * MAX(0,\ 0.886389092 - SHGC) - \\ & 863.890400672877 * MAX(0,\ WGR - 0.45) - 1103.7045035935 * MAX(0,\ 0.45 - WGR) - \\ & 85.8440109482611 * MAX(0,\ OPF - 0.691211326) + 366.519326786153 * \\ & MAX(0,\ 0.691211326 - OPF) - 3.1233303730001 * MAX(0,\ EOA - 10.07410732) + \\ & 1.38045002272926 * MAX(0,\ BO - 71) + 3.74988005950721 * MAX(0,\ 71 - BO) - \\ & 9.98450663115512 * MAX(0,\ BO - 302) + 12.8413905906219 * MAX(0,\ BO - 292) - \\ & 2.9250134400962 * MAX(0,\ BO - 198) + 216.270305178486 * MAX(0,\ SHGC - 0.584244224) \end{aligned} \tag{25}$$

With the application of MARS, the natural ventilation prediction model is expressed by Eq. (26). The equation consists of 22 basis functions with an interaction order of three, indicating the product of three basis functions can be treated as one equation item. The equation involves one more predictor compared to Eq. (25). R^2 of the model is improved from 0.926 to 0.970, while RMSE is decreased from 2.570 to 1.647.

$$\begin{aligned} ACR = {} & 44.9459619161843 + 51.9195905077679*MAX(0,\ WGR-0.45) - 86.4205450763241* \\ & MAX(0,\ 0.45-WGR) - 96.1347320579793*MAX(0,\ SHGC-0.880388966) - 32.4142971265033* \\ & MAX(0,\ 0.880388966-SHGC) + 0.541355944145259*MAX(0,\ IAMFC-5.220064518) - 0.916957447015047* \\ & MAX(0,\ 5.220064518-IAMFC) + 67.5296093913248*MAX(0,\ 0.855157446-SHGC)*MAX(0,\ 0.45-WGR) - \\ & 0.0449041687359502*MAX(0,\ EOA-10.07410732) - 3.31145260618196*MAX(0,\ OPF-0.325849724) + \\ & 15.050374361212*MAX(0,\ 0.325849724-OPF) + 9.0863517340684*MAX(0,\ 0.45-WGR)* \\ & MAX(0,\ OPF-0.452537422) - 28.9751417976488*MAX(0,\ 0.45-WGR)*MAX(0,\ 0.452537422-OPF) + \\ & 0.00591277715537106*MAX(0,\ BO-71) + 0.0307598086343345*MAX(0,\ 71-BO) - 0.175367435878637* \\ & MAX(0,\ WU-1.439781962) + 1.38198969226282*MAX(0,\ 1.439781962-WU) + 2.64104065922396* \\ & MAX(0,\ 0.855157446-SHGC)*MAX(0,\ 0.45-WGR)*MAX(0,\ 7.554237721-IAMFC) \end{aligned} \tag{26}$$

The MARS model for thermal comfort is then built as Eq. (27). The formula exploits the same number of inputs as Eq. (26) with a different parameter selection. The number of basis functions is 29, most complicated among three models. RMSE is reduced to 0.022 from the original 0.025, while R^2 increases from 0.871 to 0.901. Predictions by the thermal comfort and natural ventilation models can correlate closely with respective simulated results as shown in Fig. 17. A detailed comparison of

model trainings with the linear and MARS methods is summarized in Table 6. Although GCVs use a formula to approximate the estimation error in a similar way of leave-one-out validation, a cross-validation with a separate test dataset is still performed on both the linear regression model and MARS model, as presented in Table 7.

$$
\begin{aligned}
ACT = {} & 0.351560468221603 + 1.48846224940798*MAX(0, SHGC-0.886389092) + \\
& 0.297315059821451*MAX(0, 0.886389092-SHGC) + 0.26468850497766*MAX(0, 0.45-WGR) + \\
& 0.00058520471879665 3*MAX(0, EOA-10.07410732) + 0.0307841215154603* \\
& MAX(0, OPF-0.325849724) - 0.139296739328028*MAX(0, 0.325849724-OPF) - 0.112395869005712* \\
& MAX(0, 0.45-WGR)*MAX(0, WTR-0.480050694) + 0.241444642964237*MAX(0, 0.45-WGR)* \\
& MAX(0, 0.480050694-WTR) + 0.449002634030455*MAX(0, SHGC-0.407346141)*MAX(0, 0.45-WGR)* \\
& MAX(0, WTR-0.480050694) - 0.0017587596249228*MAX(0, 0.886389092-SHGC)*MAX(0, BO-292) - \\
& 0.00012293308196942 4*MAX(0, 0.886389092-SHGC)*MAX(0, 292-BO) - 0.0713021158065392* \\
& MAX(0, 0.45-WGR)*MAX(0, OPF-0.452537422) + 0.221322416837747*MAX(0, 0.45-WGR)* \\
& MAX(0, 0.452537422-OPF) + 0.00112687834238276*MAX(0, WU-1.439781962) - \\
& 0.0184281687611045*MAX(0, 1.439781962-WU) + 0.00016016718666004* \\
& MAX(0, 0.886389092-SHGC)*MAX(0, EOA-70.13825301)*MAX(0, BO-292) + \\
& 0.00001966384613191 91*MAX(0, 0.886389092-SHGC)*MAX(0, 70.13825301-EOA)*MAX(0, BO-292)
\end{aligned}
\tag{27}
$$

As suggested by existing literatures [29], RMSE of a training dataset, or alternatively called the apparent error, tends to underestimate the uncertainty of a test dataset due to statistical overfitting. This situation is consolidated by increased RMSE for natural ventilation and thermal comfort models. However, RMSE of the daylight model from the test dataset suggests an uncommon increase of precision, which is a different finding from a similar statistical study on the model selection between the MARS and the linear regression [28]. Regarding with the MARS model for the daylight performance, more sophisticated machine learning methods such as the artificial neural network might be employed to further promote the prediction accuracy [32]. In addition, obtained meta-models from this statistical modeling process can be used for calculating the indoor environmental conditions instead of a more complicated simulation software to promote the computation efficiency. Based on the calculated daylight illuminance level and a preset control threshold the total hours requiring artificial lighting can be determined. Furthermore, the required mechanical cooling hours can also be deduced from the thermal discomfort time according to the comfort index. As a result, important design parameters and transformed model outputs derived from this research can be incorporated in a multi-objective optimization process to determine the optimum building design in an early planning stage of any green building project [8, 59, 60].

4. Conclusions and recommendations for future work

Green building schemes encourage the application of passive design strategies in the early design stage of building projects. The passive design can reduce building energy consumption and provide quality indoor environmental conditions with natural lighting and ventilation by appropriately controlling design parameters of the building layout, envelope thermophysics, building geometry and air-tightness. In this paper, sensitivity analyses and statistical modelling are performed on a typical high-rise residential building in hot and humid climates to investigate the impact of the sampling size, effectiveness of rank transformations, uncertainty of sensitivity indices and precision of different meta-models. Main conclusions can be drawn as below:

1) The multiple linear regression has comparative advantages in sensitivity analyses due to its structural simplicity and flexibility. However, the sensitivity indices (SRC and SRRC), prediction error (RMSE) and goodness of fit (R^2) can vary greatly over different sample sizes. In this research, a large sample size over 100 per regression coefficient is determined for acquiring stable statistical estimations form regression models of selected passive design parameters and indoor environmental indices.
2) Residual plots with smooth fit curves identified the non-linearity and deviations from the normality assumption in the developed linear regression model. Therefore, rank transformations of model responses were performed to calibrate sensitivity coefficients (SRRCs), which were modified by up to 6% leading to a change of rankings in the relative importance of design parameters. The window transmittance property (SHGC/VLT) and window to ground ratio are determined to be the two most influential factors over the daylight, natural ventilation and thermal comfort performance in hot and humid climates.
3) The bootstrap method was applied to estimate the confidence interval of sensitivity indices. An adequate bootstrap replication of 1000 samples was determined based on the stability of unstandardized regression coefficient for each design factor. Standard deviations of all SRRCs for the three regression models are proved to be within 2%.
4) RMSE and R^2 of linear regression models are further improved by introducing the non-parametric regression analysis. Both natural ventilation and thermal comfort MARS models are closely fitted with chosen predictors (R^2 of 0.970 and 0.901) and can produce acceptable prediction uncertainties within 1.796 (air change rate) and 0.023 (thermal comfort time ratio)

589 respectively. The daylight performance model can be further refined by applying a more complex
590 machine learning approach such as the artificial neural network.
591 Investigated indoor environmental indices in this research can be linked to potential building
592 energy consumption in cooling and lighting. Therefore, identified important design parameters and
593 transformed model outputs can be incorporated in a multi-objective optimization process to determine
594 the optimum building design by considering the synergy of the energy efficiency and indoor
595 environment quality. The derived robust sensitivity indices can also be used to compose a
596 comprehensive weighting system for the passive design assessment approach in current green
597 building schemes. Besides, after a further refinement of the prediction accuracy, developed meta-
598 models can substitute the complicated simulation software to improve the computation efficiency and
599 offer reliable predictions of building performances in an early design stage.
600

601 ## Acknowledgment

602 The work described in this paper was supported by the Hong Kong PhD Fellowship Scheme, the
603 Construction Industry Council of Hong Kong and the Research Institute for Sustainable Urban
604 Development (RISUD) of The Hong Kong Polytechnic University. Appreciation is also given to the
605 Housing Authority of the Hong Kong SAR Government as well as the Shenzhen Peacock Plan
606 (KQTD20150716164422 25) for supporting our research project in built environment studies.
607

608 ## Nomenclatures

Abbreviation	
ACR	Air change rate
ACT	ASHRAE55 Comfort Time
BEAM	building environment assessment method
BO	building orientation
ENP	effective number of parameters
EOA	external obstruction angle
GCV	generalized cross validation
HVAC	heating ventilation and air conditioning
IAMFC	infiltration air mass flow coefficient
IL	illuminance level
LHS	Latin hypercube sampling
MARS	multivariate adaptive regression splines
MSE	mean squared error
OPF	overhang projection fraction
PRH	public rental housing
RMSE	root mean square error
SA	sensitivity analysis

SHGC	solar heat gain coefficient
SRC	standardized regression coefficient
SRRC	standardized rank regression coefficient
VIF	variance inflation factor
VLT	visible light transmittance
WGR	window to ground ratio
WSH	wall specific heat
WTR	wall thermal resistance

References

[1] Lee WL. A comprehensive review of metrics of building environmental assessment schemes. Energy and Buildings. 2013;62:403-13.

[2] Campaniço H, Hollmuller P, Soares PMM. Assessing energy savings in cooling demand of buildings using passive cooling systems based on ventilation. Applied Energy. 2014;134:426-38.

[3] Eicker U. Cooling strategies, summer comfort and energy performance of a rehabilitated passive standard office building. Applied Energy. 2010;87:2031-9.

[4] Fong KF, Lee CK. Towards net zero energy design for low-rise residential buildings in subtropical Hong Kong. Applied Energy. 2012;93:686-94.

[5] Lee WL, Yik FWH, Burnett J. Assessing energy performance in the latest versions of Hong Kong Building Environmental Assessment Method (HK-BEAM). Energy and Buildings. 2007;39:343-54.

[6] Wong JK-W, Kuan K-L. Implementing 'BEAM Plus' for BIM-based sustainability analysis. Automation in Construction. 2014;44:163-75.

[7] Deru M, Enck, J., Grumman, D., Haggans, M., Larsson, N., McCarry, B., Rosenbaum, M. and Turner. The Design Process—Early Stages. In: Grumman D, editor. The ASHRAE GreenGuide. Atlanta: American Society of Heating, Refrigerating, and Air-Conditioning Engineers, Inc.; 2003. p. 27.

[8] BEAM. BEAM Plus New Buildings Version 1.2. HKGBC and BEAM Society Limited. 2012.

[9] Chen X, Yang H, Lu L. A comprehensive review on passive design approaches in green building rating tools. Renewable and Sustainable Energy Reviews. 2015;50:1425-36.

[10] Chen X, Yang H, Zhang W. A comprehensive sensitivity study of major passive design parameters for the public rental housing development in Hong Kong. Energy. 2015;93:1804-18.

[11] Huang K-T, Hwang R-L. Future trends of residential building cooling energy and passive adaptation measures to counteract climate change: The case of Taiwan. Applied Energy.

[12] Mangkuto RA, Rohmah M, Asri AD. Design optimisation for window size, orientation, and wall reflectance with regard to various daylight metrics and lighting energy demand: A case study of buildings in the tropics. Applied Energy. 2016;164:211-9.

[13] Tian W. A review of sensitivity analysis methods in building energy analysis. Renewable and Sustainable Energy Reviews. 2013;20:411-9.

[14] Ascione F, Bianco N, De Stasio C, Mauro GM, Vanoli GP. Multi-stage and multi-objective optimization for energy retrofitting a developed hospital reference building: A new approach to assess cost-optimality. Applied Energy. 2016;174:37-68.

[15] Méndez Echenagucia T, Capozzoli A, Cascone Y, Sassone M. The early design stage of a

building envelope: Multi-objective search through heating, cooling and lighting energy performance analysis. Applied Energy. 2015;154:577-91.
[16] Domínguez-Muñoz F, Cejudo-López JM, Carrillo-Andrés A. Uncertainty in peak cooling load calculations. Energy and Buildings. 2010;42:1010-8.
[17] Lam JC, Hui SCM. Sensitivity analysis of energy performance of office buildings. Building and Environment. 1996;31:27-39.
[18] Qian J. Towards a Whole-life Value Optimisation Model for Facade Design: University of Cambridge; 2013.
[19] Wang L-S, Ma P, Hu E, Giza-Sisson D, Mueller G, Guo N. A study of building envelope and thermal mass requirements for achieving thermal autonomy in an office building. Energy and Buildings. 2014;78:79-88.
[20] Lam JC, Li DHW. An analysis of daylighting and solar heat for cooling-dominated office buildings. Solar Energy. 1999;65:251-62.
[21] Chan ALS. Effect of adjacent shading on the thermal performance of residential buildings in a subtropical region. Applied Energy. 2012;92:516-22.
[22] Han Y, Taylor JE, Pisello AL. Exploring mutual shading and mutual reflection inter-building effects on building energy performance. Applied Energy.
[23] Breesch H, Janssens A. Performance evaluation of passive cooling in office buildings based on uncertainty and sensitivity analysis. Solar Energy. 2010;84:1453-67.
[24] Yildiz Y, Korkmaz K, Göksal Özbalta T, Durmus Arsan Z. An approach for developing sensitive design parameter guidelines to reduce the energy requirements of low-rise apartment buildings. Applied Energy. 2012;93:337-47.
[25] Yıldız Y, Arsan ZD. Identification of the building parameters that influence heating and cooling energy loads for apartment buildings in hot-humid climates. Energy. 2011;36:4287-96.
[26] Gao CF, Lee WL. Evaluating the influence of openings configuration on natural ventilation performance of residential units in Hong Kong. Building and Environment. 2011;46:961-9.
[27] Chu C-R, Chiu YH, Tsai Y-T, Wu S-L. Wind-driven natural ventilation for buildings with two openings on the same external wall. Energy and Buildings. 2015;108:365-72.
[28] Tian W, Song J, Li Z, de Wilde P. Bootstrap techniques for sensitivity analysis and model selection in building thermal performance analysis. Applied Energy. 2014;135:320-8.
[29] Tian W, Choudhary R, Augenbroe G, Lee SH. Importance analysis and meta-model construction with correlated variables in evaluation of thermal performance of campus buildings. Building and Environment. 2015;92:61-74.
[30] Shin M, Do SL. Prediction of cooling energy use in buildings using an enthalpy-based cooling degree days method in a hot and humid climate. Energy and Buildings. 2016;110:57-70.
[31] Hilliard T, Swan L, Kavgic M, Qin Z, Lingras P. Development of a whole building model predictive control strategy for a LEED silver community college. Energy and Buildings. 2016;111:224-32.
[32] Melo AP, Fossati M, Versage RS, Sorgato MJ, Scalco VA, Lamberts R. Development and analysis of a metamodel to represent the thermal behavior of naturally ventilated and artificially air-conditioned residential buildings. Energy and Buildings. 2016;112:209-21.
[33] Fan C, Xiao F, Wang S. Development of prediction models for next-day building energy consumption and peak power demand using data mining techniques. Applied Energy. 2014;127:1-10.

690 [34] Zhao M, Künzel HM, Antretter F. Parameters influencing the energy performance of residential
691 buildings in different Chinese climate zones. Energy and Buildings. 2015;96:64-75.
692 [35] Zhai Z, Johnson M-H, Krarti M. Assessment of natural and hybrid ventilation models in
693 whole-building energy simulations. Energy and Buildings. 2011;43:2251-61.
694 [36] Schulze T, Eicker U. Controlled natural ventilation for energy efficient buildings. Energy and
695 Buildings. 2013;56:221-32.
696 [37] ENERGYPLUS™. EnergyPlus Engineering Reference - The Reference to EnergyPlus
697 Calculations: US Department of Energy; 2013.
698 [38] Walton GN. AIRNET – A Computer Program for Building Airflow Network Modeling.
699 National Institute of Standards and Technology, Gaithersburg, Maryland; 1989.
700 [39] ASHRAE. ASHRAE 55-2004: Thermal Environmental Conditions for Human Occupancy.
701 Atlanta2004.
702 [40] Haase M, Amato A. An investigation of the potential for natural ventilation and building
703 orientation to achieve thermal comfort in warm and humid climates. Solar Energy.
704 2009;83:389-99.
705 [41] Qi R, Lu L, Huang Y. Energy performance of solar-assisted liquid desiccant air-conditioning
706 system for commercial building in main climate zones. Energy Conversion and Management.
707 2014;88:749-57.
708 [42] Lam JC, Tang HL, Li DHW. Seasonal variations in residential and commercial sector
709 electricity consumption in Hong Kong. Energy. 2008;33:513-23.
710 [43] Chen X, Yang H. Combined thermal and daylight analysis of a typical public rental housing
711 development to fulfil green building guidance in Hong Kong. Energy and Buildings.
712 2015;108:420-32.
713 [44] Lam JC. Residential sector air conditioning loads and electricity use in Hong Kong. Energy
714 Conversion and Management. 2000;41:1757-68.
715 [45] Mavromatidis LE, Marsault X, Lequay H. Daylight factor estimation at an early design stage to
716 reduce buildings' energy consumption due to artificial lighting: A numerical approach based on
717 Doehlert and Box–Behnken designs. Energy. 2014;65:488-502.
718 [46] Li DHW, Wong SL, Tsang CL, Cheung GHW. A study of the daylighting performance and
719 energy use in heavily obstructed residential buildings via computer simulation techniques.
720 Energy and Buildings2006. p. 1343-8.
721 [47] Robert CP, Casella G. Monte Carlo Statistical Methods: Springer; 2004.
722 [48] Kim K, von Spakovsky MR, Wang M, Nelson DJ. A hybrid multi-level optimization approach
723 for the dynamic synthesis/design and operation/control under uncertainty of a fuel cell system.
724 Energy. 2011;36:3933-43.
725 [49] Loutzenhiser PG, Maxwell GM, Manz H. An empirical validation of the daylighting
726 algorithms and associated interactions in building energy simulation programs using various
727 shading devices and windows. Energy. 2007;32:1855-70.
728 [50] Calleja Rodríguez G, Carrillo Andrés A, Domínguez Muñoz F, Cejudo López JM, Zhang Y.
729 Uncertainties and sensitivity analysis in building energy simulation using macroparameters.
730 Energy and Buildings. 2013;67:79-87.
731 [51] PALLANT J. SPSS Survival Manual - A step by step guide to data analysis using SPSS for
732 Windows: Allen & Unwin; 2002.
733 [52] Naji S, Keivani A, Shamshirband S, Alengaram UJ, Jumaat MZ, Mansor Z, et al. Estimating

building energy consumption using extreme learning machine method. Energy. 2016;97:506-16.
[53] Saltelli A, Sobol IM. About the use of rank transformation in sensitivity analysis of model output. Reliability Engineering & System Safety. 1995;50:225-39.
[54] Efron B, Tibshirani R. An introduction to the bootstrap: Chapman & Hall Inc.; 1993.
[55] James G, Witten D, Hastie T, Tibshirani R. An Introduction to Statistical Learning with Application in R: Springer; 2013.
[56] CHERNICK MR. Bootstrap Methods: A Guide for Practitioners and Researchers. 2nd ed: Wiley-Interscience; 2007.
[57] Tabachnick BG, & Fidell, L. S. Using Multivariate Statistics: New York: HarperCollins; 2007.
[58] Storlie CB, Swiler LP, Helton JC, Sallaberry CJ. Implementation and evaluation of nonparametric regression procedures for sensitivity analysis of computationally demanding models. Reliability Engineering & System Safety. 2009;94:1735-63.
[59] LEED. LEED Reference Guide for Building Design and Construction 2013 Edition, Leadership in Energy and Environmental Design Program. US Green Building Council. 2013.
[60] Chen X, Yang H, Sun K. A holistic passive design approach to optimize indoor environmental quality of a typical residential building in Hong Kong. Energy. 2016;113:267-81.

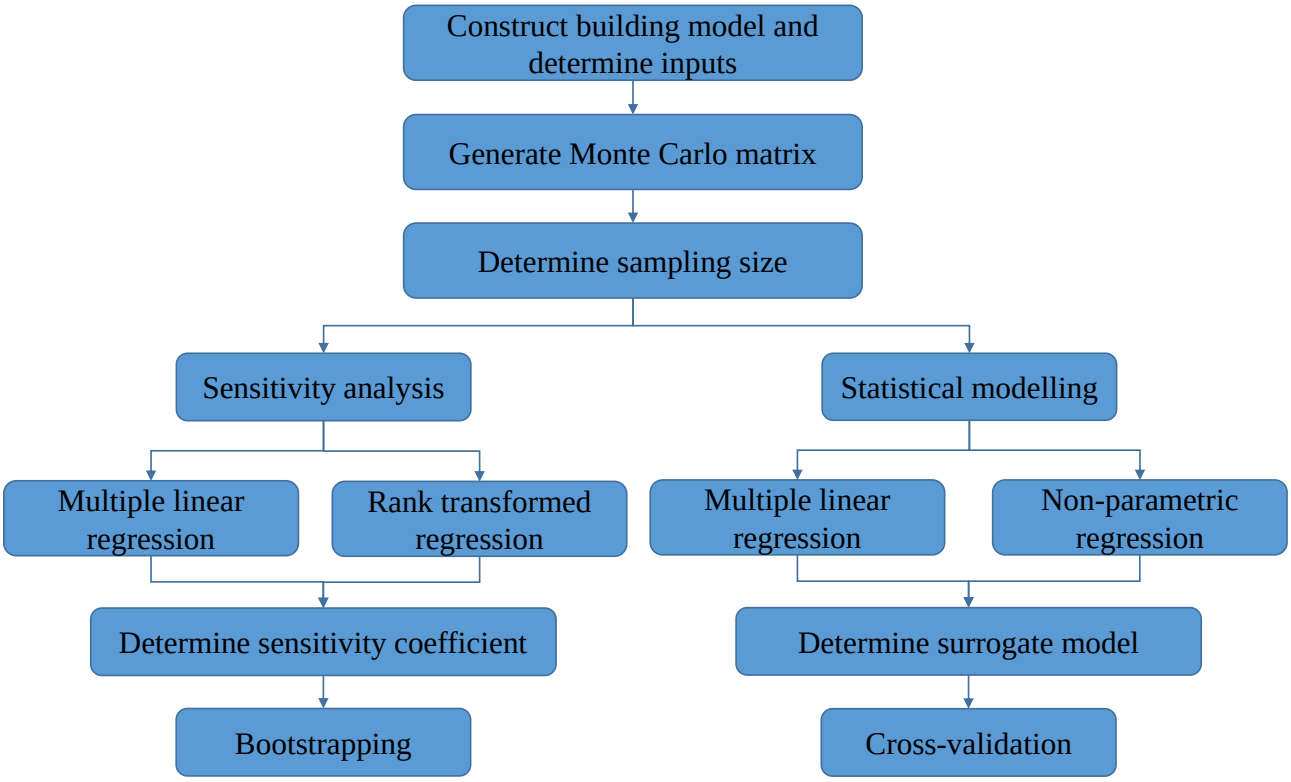

Fig. 1 Proposed flowchart of research methodology

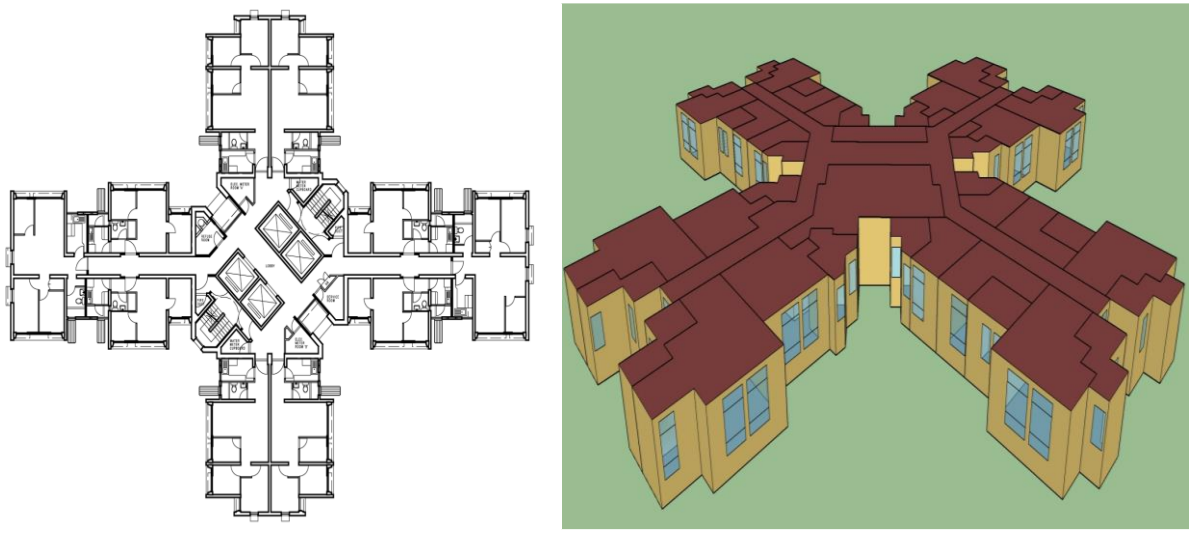

Fig.2 Standard typical floor layout plan and 3D model in EnergyPlus

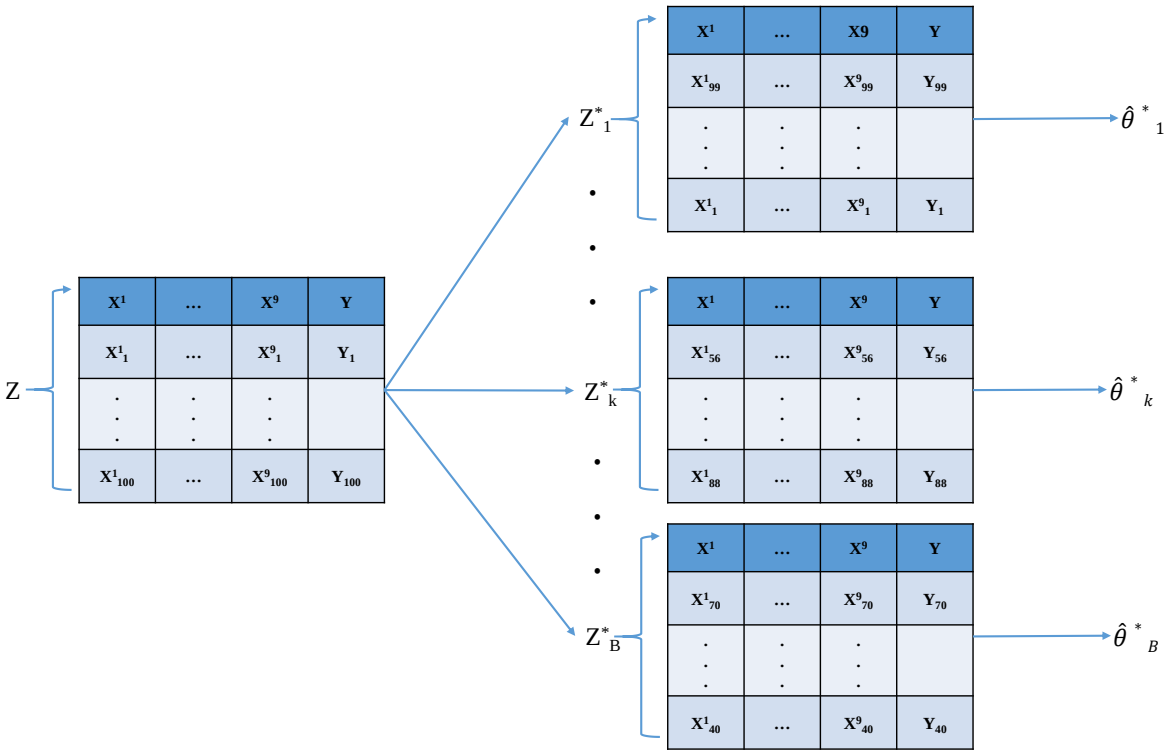

Fig. 3 Flowchart of bootstrapping

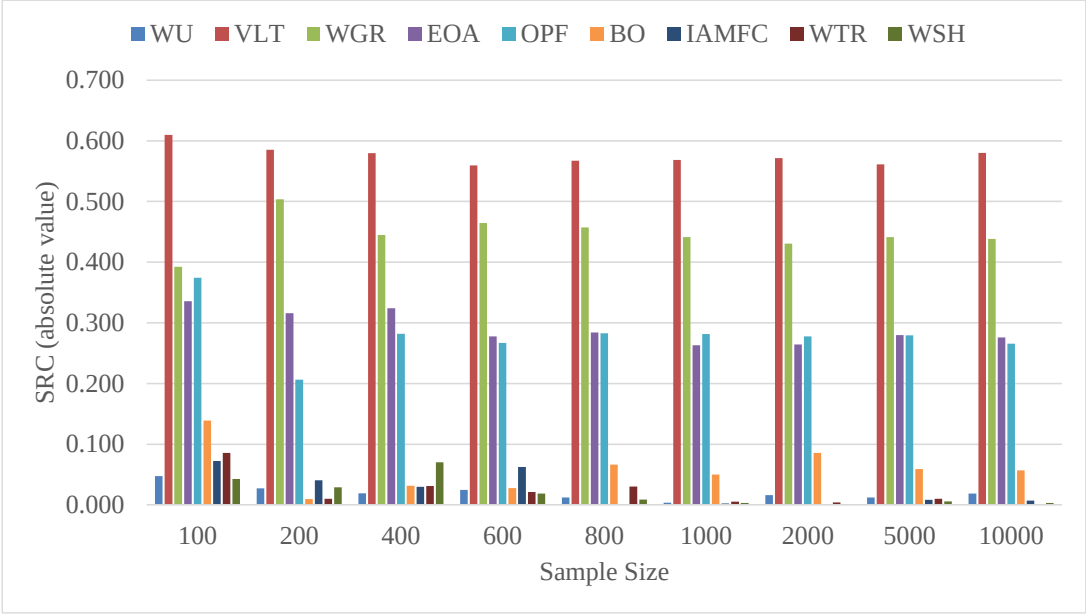

Fig. 4 Variation of SRCs (absolute value) with the sampling size for illuminance level

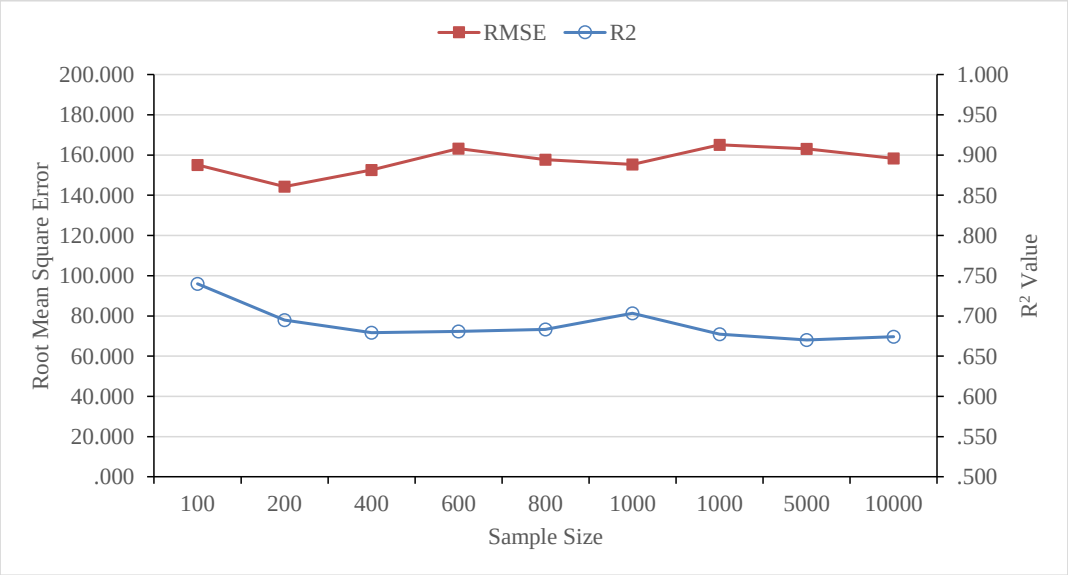

Fig. 5 Variation of R^2 and RMSE with the sampling size for the illuminance level

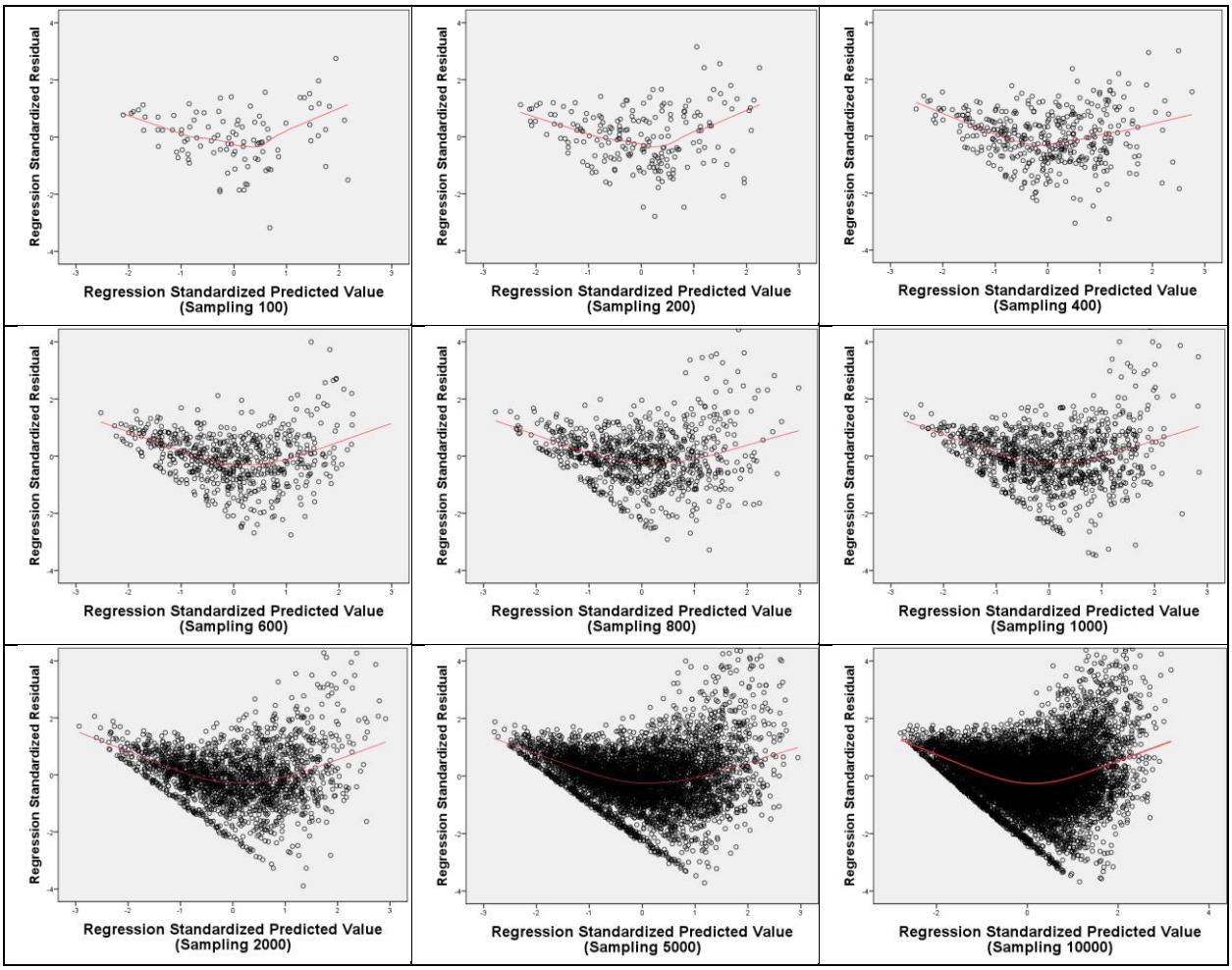

Fig. 6 Residual scatterplots with different sampling sizes for the illuminance level

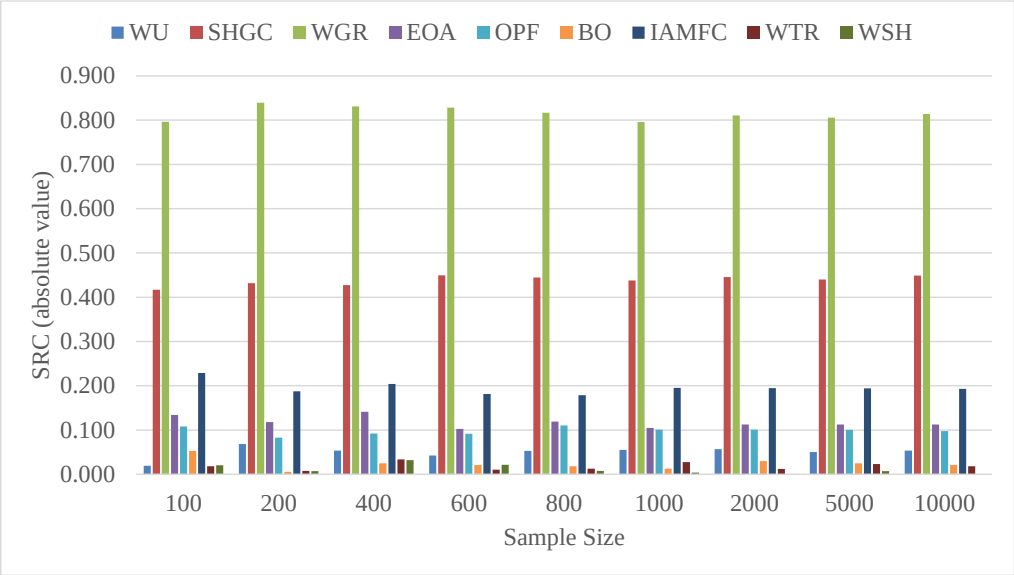

Fig. 7 Variation of SRCs (absolute value) with the sampling size for the air change rate

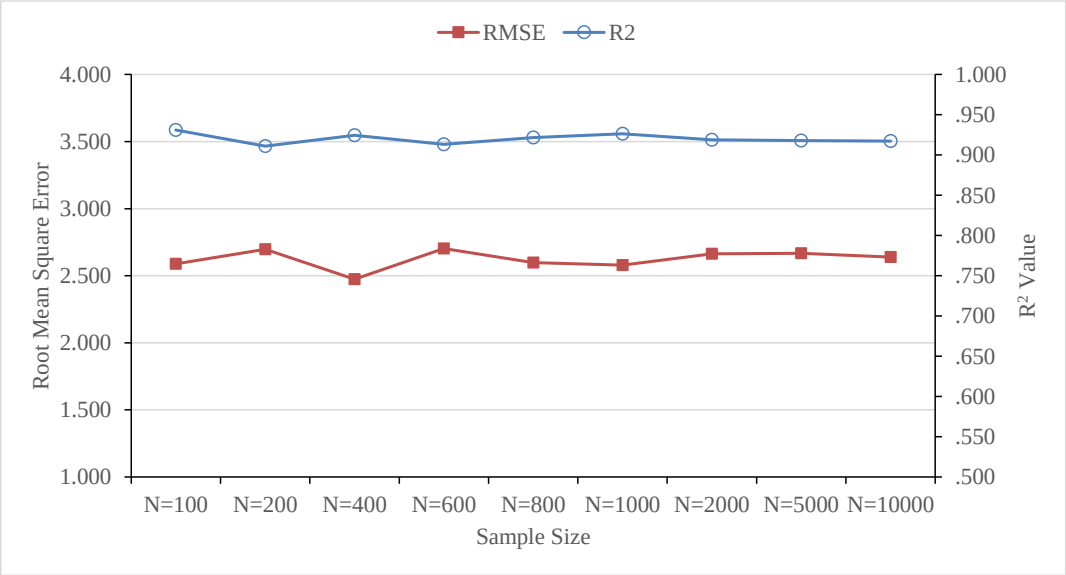

Fig. 8 Variation of R^2 and RMSE with the sampling size for the air change rate

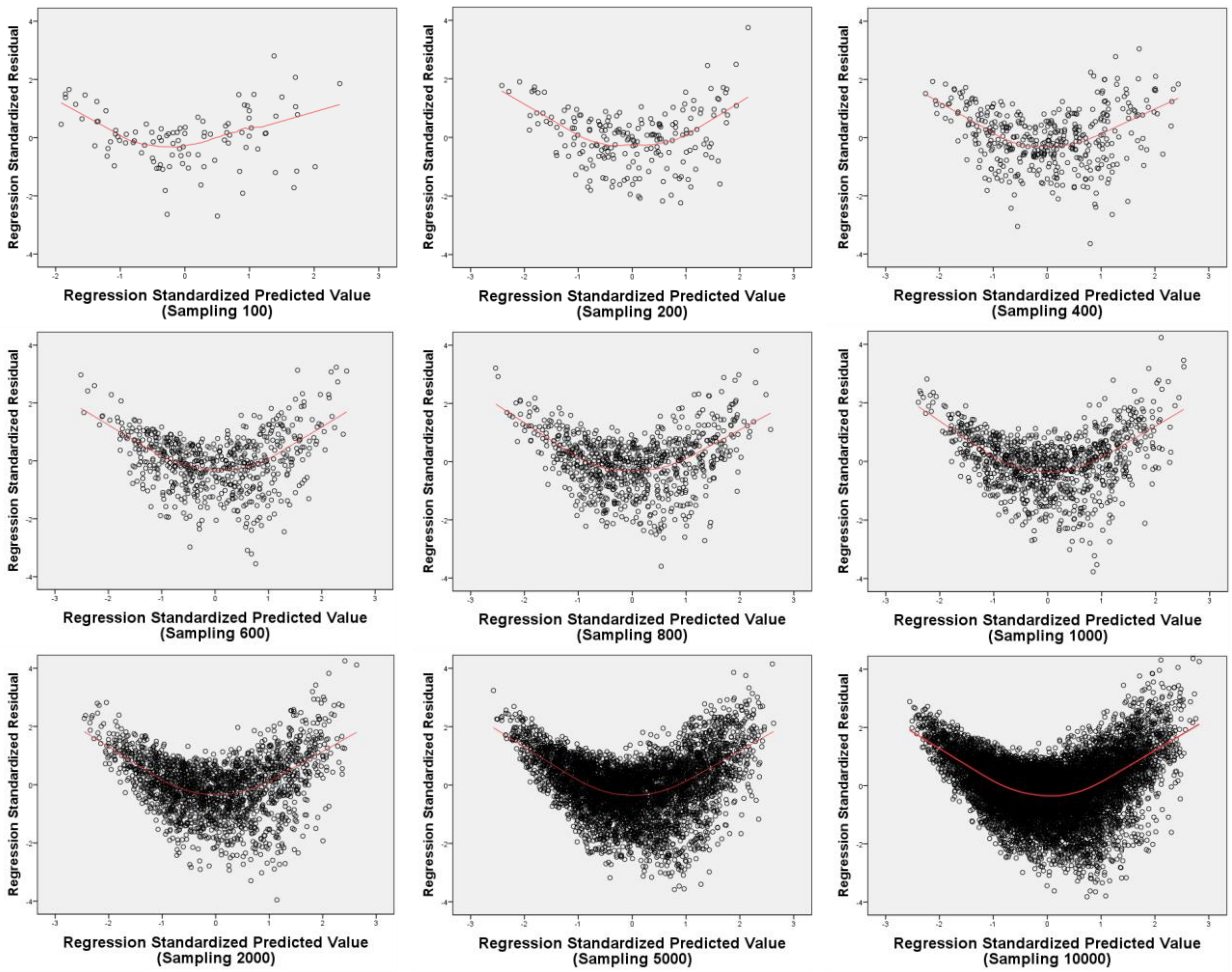

Fig. 9 Residual scatterplots with different sampling sizes for the air change rate

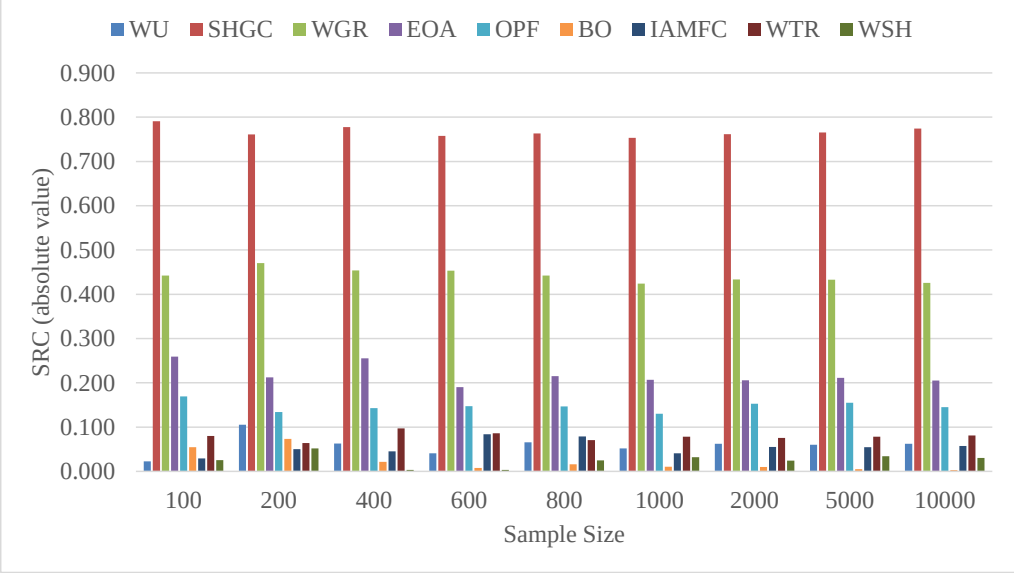

Fig. 10 Variation of SRCs (absolute value) with the sampling size for the ASHRAE55 comfort time

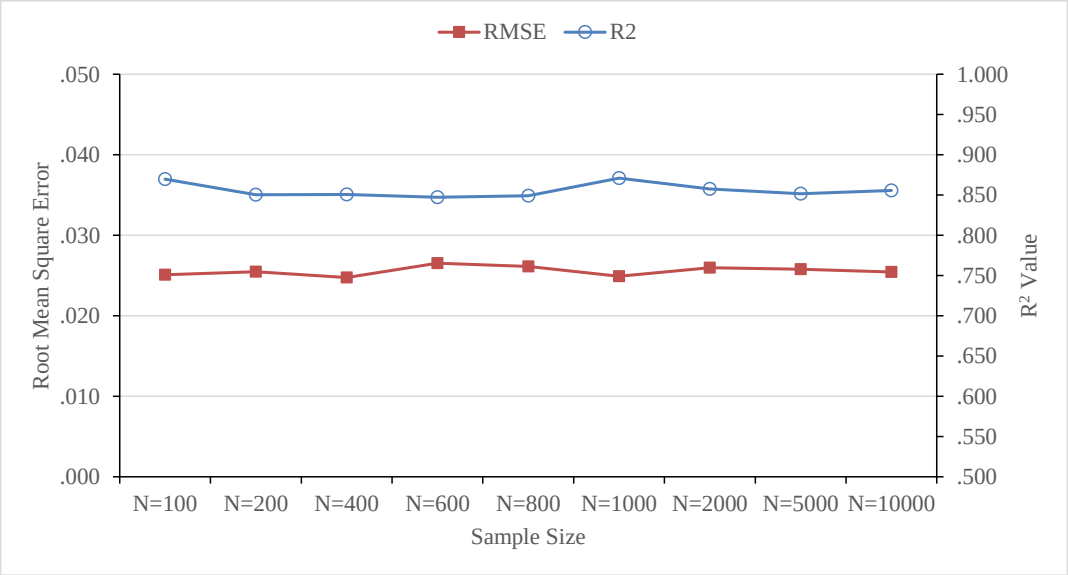

Fig. 11 Variation of R^2 and RMSE with the sampling size for the ASHRAE55 comfort time

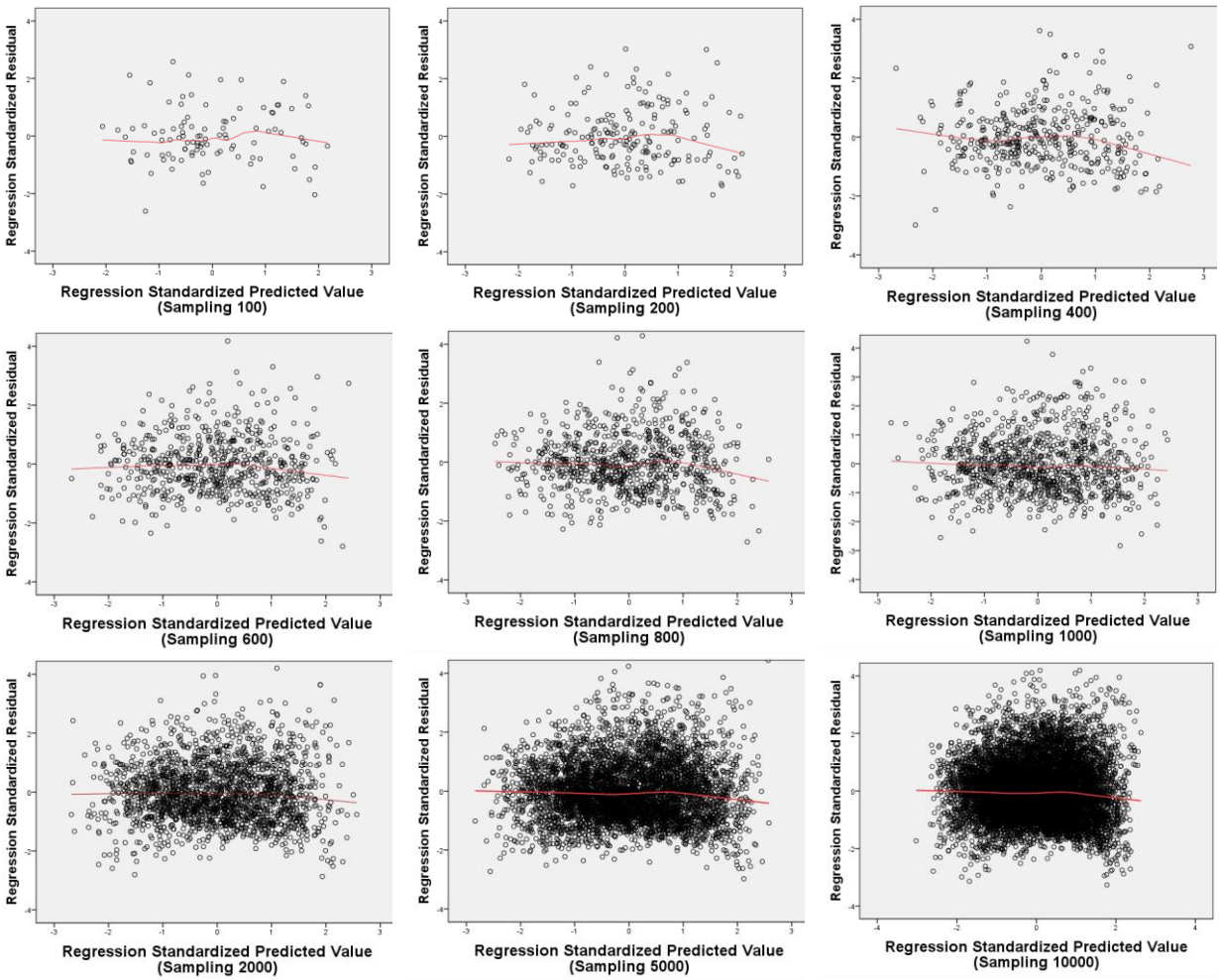

Fig. 12 Residual scatterplots with different sampling sizes for the ASHRAE55 comfort time

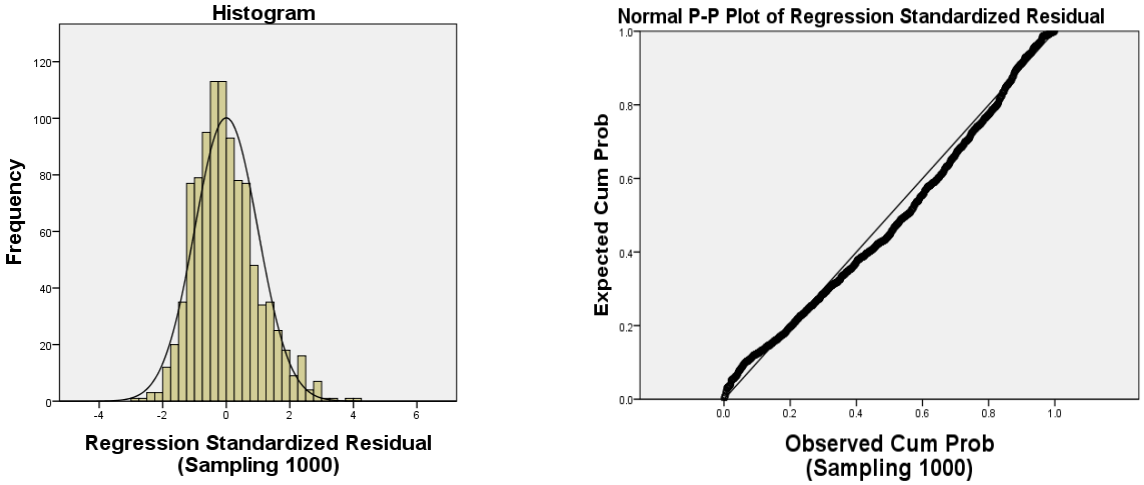

Fig. 13 Residual plots for the ASHRAE55 comfort time with a sample size of 1000

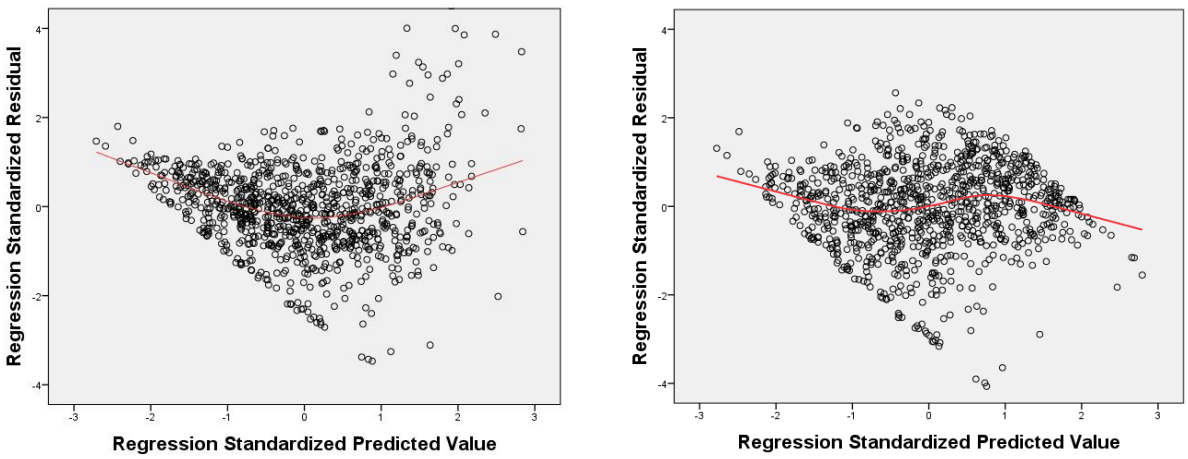

a. Original model b. Rank transformed model

Fig. 14 Residual plots for original and rank transformed data for the illuminance level

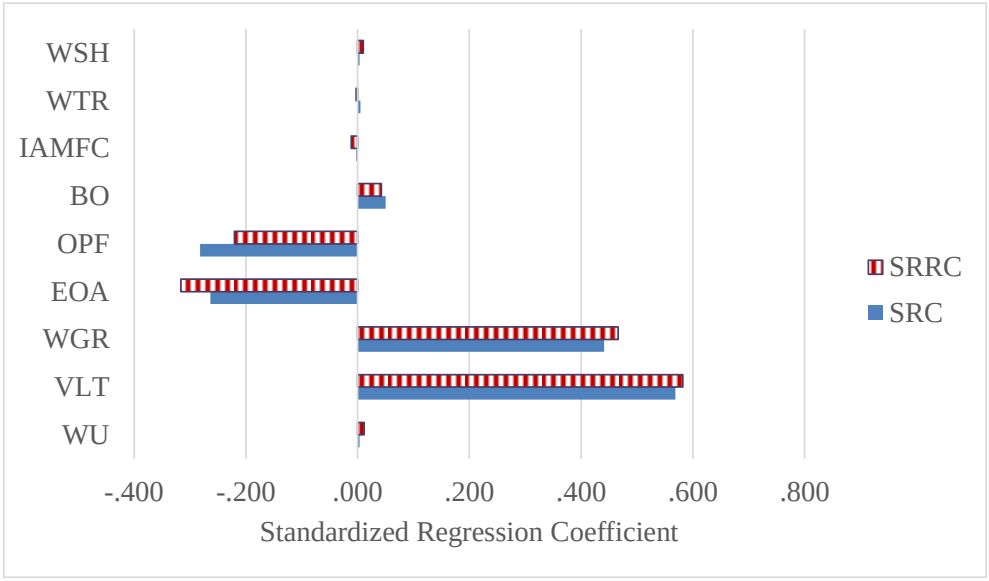

Fig. 15 Variation of sensitivity coefficients with rank transformations of the illuminance level

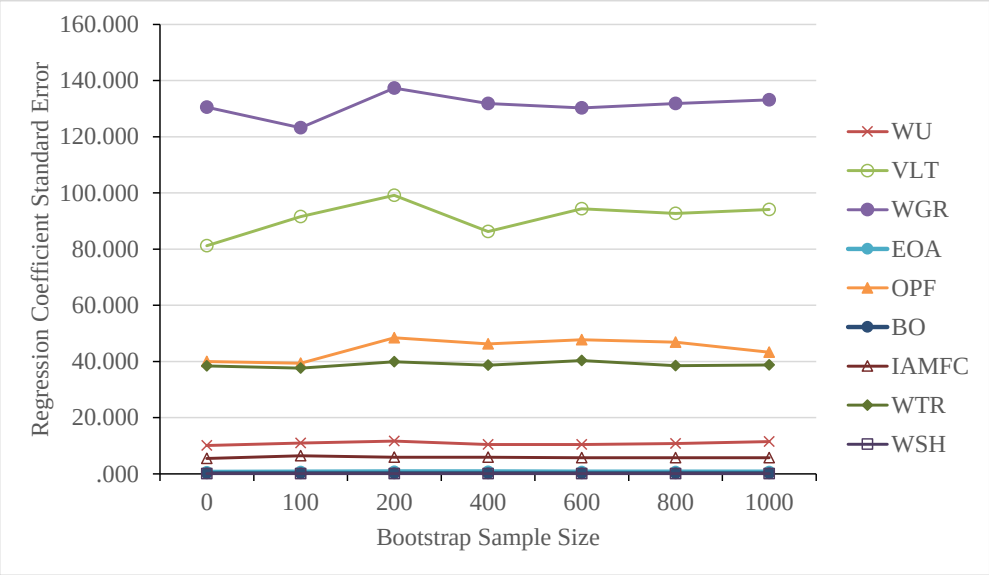

Fig. 16 Variation of regression coefficient standard error versus bootstrap sample sizes

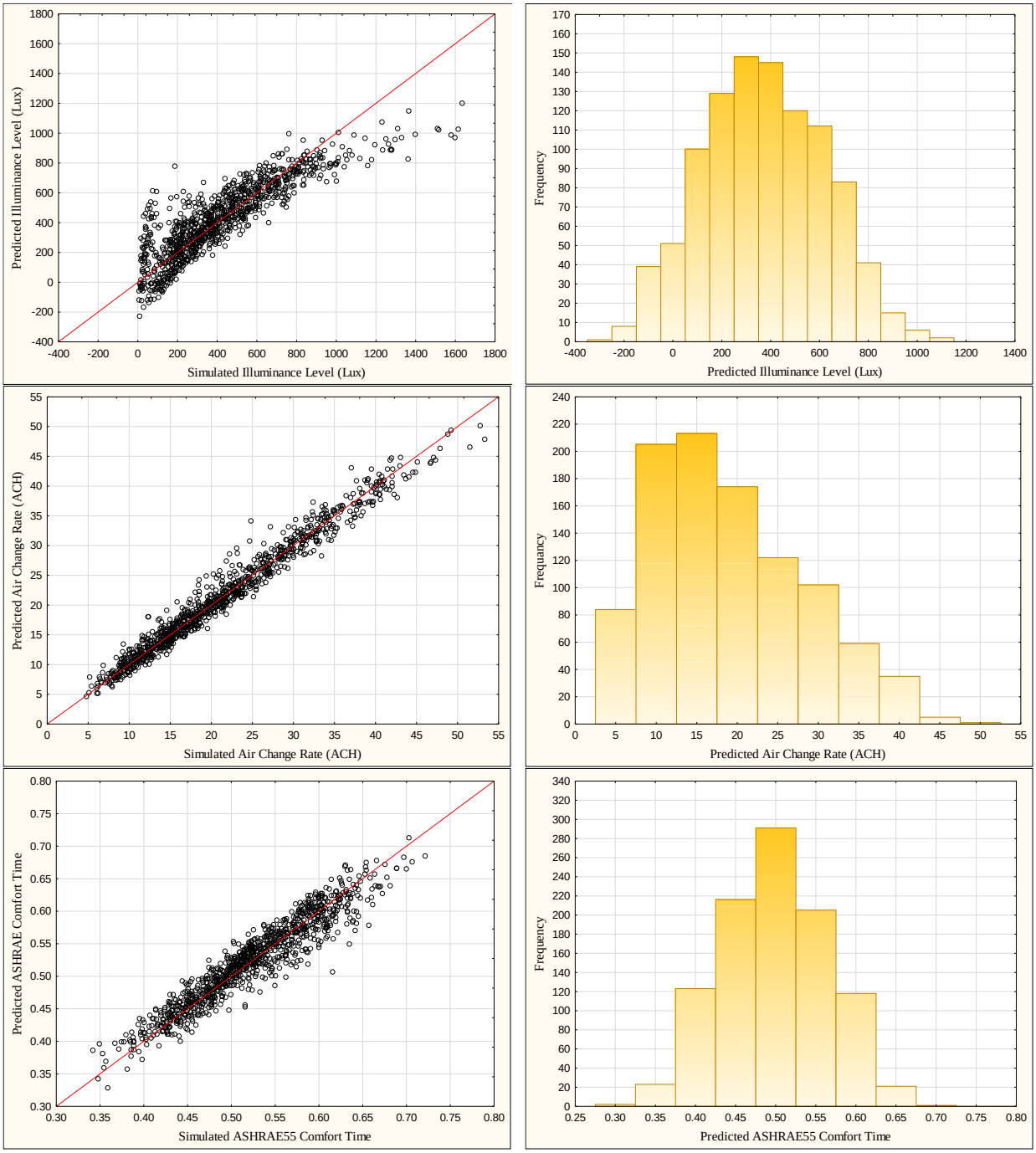

Fig. 17 The relation between predicted and simulated results and distribution of outputs for MARS models

Table 1 Building physics of the baseline generic model

Parameter		Unit	Value
Building Layout	Floor Area	m^2	23.2 (4.8×4.8)
	Height	m	2.7
	Orientation	-	West
Obstruction/Shading	Obstruction Angle	°	0
	Overhang Projection fraction	-	0
External Wall	Thermal Resistance	m^2 K/W	0.09
	Specific Heat	J/kg K	840
	Solar Absorptance	-	0.60
Fenestration/Window	U-Value	W/m^2 K	5.69
	Solar Heat Gain Coefficient	-	0.57
	Window to Wall Ratio	-	0.40

Table 2 Input variation and distribution

Input variables	Unit	Probability	Range
Building orientation (BO)	°	Continuous Uniform	0 - 360
External obstruction angle (EOA)	°	Continuous Uniform	0 - 87
External wall thermal resistance (WTR)	m^2 K/W	Continuous Uniform	0.09 - 1.85
External wall specific heat (WSH)	J/kg K	Continuous Uniform	800 - 1800
Window solar heat gain coefficient (SHGC)	-	Continuous Uniform	0.2 - 0.9
Window U-value (WU)	W/m^2 K	Continuous Uniform	0.5 - 6.0
Window to ground ratio (WGR)	-	Continuous Uniform	0.10 - 0.50
Overhang projection fraction (OPF)	-	Continuous Uniform	0.00 – 0.56
Infiltration air mass flow coefficient (IAMFC)	kg/s	Continuous Uniform	0.00 – 0.03

Table 3 Comparison of SRCs and SRRCs for the three regression models

Output	Illuminance Level		Air Change Rate		ASHRAE55 Comfort Time	
	SRC	SRRC	SRC	SRRC	SRC	SRRC
WU	0.004	0.012	-0.055	-0.035	0.052	0.047
SHGC/VLT	0.569	0.582	0.438	0.422	-0.753	-0.764
WGR	0.441	0.466	0.796	0.817	-0.424	-0.418
EOA	-0.263	-0.316	-0.105	-0.116	0.207	0.207
OPF	-0.282	-0.221	-0.101	-0.081	0.130	0.123
BO	0.050	0.042	0.012	0.019	0.011	0.009
IAMFC	-0.002	-0.011	0.195	0.185	0.041	0.045
WTR	0.005	-0.002	0.027	0.025	-0.078	-0.059
WSH	0.003	0.010	-0.004	0.000	0.032	0.030

Table 4 Confidence intervals of SRRCs for the sensitivity analysis

Output	Illuminance Level			Air Change Rate			ASHRAE Comfort Time		
	SRRC	95% Confidence Interval		SRRC	95% Confidence Interval		SRRC	95% Confidence Interval	
		Lower	Upper		Lower	Upper		Lower	Upper
WU	0.012	-0.020	0.043	-0.035	-0.050	-0.019	0.047	0.025	0.068
SHGC/VLT	0.582	0.549	0.615	0.422	0.404	0.438	-0.764	-0.785	-0.739
WGR	0.469	0.437	0.501	0.821	0.803	0.839	-0.421	-0.445	-0.397
EOA	-0.318	-0.356	-0.280	-0.116	-0.133	-0.098	0.208	0.182	0.233
OPF	-0.221	-0.253	-0.190	-0.081	-0.097	-0.064	0.123	0.098	0.148
BO	0.042	0.008	0.075	0.019	0.004	0.034	0.009	-0.014	0.032
IAMFC	-0.011	-0.043	0.019	0.185	0.168	0.200	0.045	0.022	0.067
WTR	-0.002	-0.034	0.032	0.025	0.009	0.041	-0.059	-0.081	-0.036
WSH	0.010	-0.023	0.041	0.000	-0.015	0.016	0.030	0.007	0.052

Table 5 Stepwise regression coefficient versus standard regression coefficient

Output	Illuminance Level		Air Change Rate		ASHRAE55 Comfort Time	
Method	Standard	Stepwise	Standard	Stepwise	Standard	Stepwise
WU	***0.004***	***0.000***	-0.055	*-0.055*	0.052	0.052
SHGC/VLT	0.569	0.568	0.438	0.438	-0.753	-0.754
WGR	0.441	0.442	0.796	0.796	-0.424	-0.424
EOA	-0.263	-0.264	-0.105	-0.105	0.207	0.206
OPF	-0.282	-0.281	-0.101	-0.101	0.130	0.130
BO	0.050	0.050	***0.012***	***0.000***	***0.011***	***0.000***
IAMFC	***-0.002***	***0.000***	0.195	0.194	0.041	0.040
WTR	***0.005***	***0.000***	0.027	0.028	-0.078	-0.078
WSH	***0.003***	***0.000***	***-0.004***	***0.000***	0.032	0.032

Table 6 Comparison between the MARS and stepwise linear model

Output	Illuminance Level		Air Change Rate		ASHRAE55 Comfort Time	
	MARS	Stepwise	MARS	Stepwise	MARS	Stepwise
R^2	0.766	0.703	0.970	0.926	0.901	0.871
RMSE	137.274	154.583	1.647	2.570	0.022	0.025
GCV	19803.200	-	2.911	-	0.0005	-

Table 7 Cross-validation with MARS and the stepwise linear model

Output	Method	RMSE	
		Training	Test
Illuminance Level	MARS	137.274	130.639
	Linear	154.583	142.395
Air Change Rate	MARS	1.647	1.796
	Linear	2.570	2.697
ASHRAE55 Comfort Time	MARS	0.022	0.023
	Linear	0.025	0.028